UNCLASSIFIED

SECURITY CLASSIFICATION OF THIS PAGE (When Data Entered)

REPORT DOCUMENTATION PAGE		READ INSTRUCTIONS BEFORE COMPLETING FORM
1. REPORT NUMBER: WHOI Contribution 6817	2. GOVT ACCESSION NO.	3. RECIPIENT'S CATALOG NUMBER
4. TITLE (and Subtitle): A LIMITED-AREA MODEL OF THE GULF STREAM: DESIGN, INITIAL EXPERIMENTS, AND MODEL-DATA INTERCOMPARISON		5. TYPE OF REPORT & PERIOD COVERED: Technical
		6. PERFORMING ORG. REPORT NUMBER: WHOI Contr. 6817
7. AUTHOR(s): J. DANA THOMPSON; W.J. SCHMITZ, JR.		8. CONTRACT OR GRANT NUMBER(s): ONR 32-05-3F, ONR 32-05-3G
9. PERFORMING ORGANIZATION NAME AND ADDRESS: Woods Hole Oceanographic Institution, Woods Hole, MA 02543		10. PROGRAM ELEMENT, PROJECT, TASK AREA & WORK UNIT NUMBERS
11. CONTROLLING OFFICE NAME AND ADDRESS: Office of Naval Research, Environmental Sciences Directorate, Arlington, VA 22217		12. REPORT DATE: September 1989
		13. NUMBER OF PAGES
14. MONITORING AGENCY NAME & ADDRESS(if different from Controlling Office)		15. SECURITY CLASS. (of this report): UNCLASSIFIED
		15a. DECLASSIFICATION/DOWNGRADING SCHEDULE

16. DISTRIBUTION STATEMENT (of this Report)

Approved for public release; Distribution unlimited

17. DISTRIBUTION STATEMENT (of the abstract entered in Block 20, if different from Report)

18. SUPPLEMENTARY NOTES

In citing this report in a bibliography the reference given should be to:

Journal of Physical Oceanography, Vol. 19, No. 6, June 1989

19. KEY WORDS (Continue on reverse side if necessary and identify by block number)

1) Gulf Stream
2) numerical model
3) eddies

20. ABSTRACT (Continue on reverse side if necessary and identify by block number)

See reverse side.

DD FORM 1 JAN 73 1473 EDITION OF 1 NOV 65 IS OBSOLETE S/N 0102-014-6601

UNCLASSIFIED

SECURITY CLASSIFICATION OF THIS PAGE (When Data Entered)

20.

A primitive-equation, n-layer, eddy-resolving circulation model has been applied to the Gulf Stream System from Cape Hatteras to east of the Grand Banks (78°–45°W, 30°–48°N). Within the limitations of the model, realistic coastlines, bottom topography, and forcing functions have been used. A two-layer version of the model was driven by observed mean climatological wind forcing and mass transport prescribed at inflow. Outflow was determined by a radiation boundary condition and an integral constraint on the mass field in each layer. Specification of a Deep Western Boundary Current (DWBC) was included in some model runs.

Six numerical experiments, from a series of over fifty integrated to statistical equilibrium, were selected for detailed description and intercomparison with observations. The basic case consisted of a flat bottom regime driven by wind forcing only. Realistic inflow transport in the upper layer was then prescribed and two different outflow specifications at the eastern boundary were studied in experiments 2 and 3. Three additional experiments involved (4) adding bottom topography (including the New England Seamount Chain), (5) adding a DWBC to experiment 4 with 20 Sv (Sv = 10^6 m^3 s^{-1}) total transport, and (6) increasing the DWBC to 40 Sv. A brief discussion of the influence of parameter variations includes modifications of dissipation (lateral eddy diffusion and bottom friction) and stratification.

Results from the sequence of experiments suggest an important role for the DWBC in determining the mean path of the Gulf Stream and consequently the distribution of eddy kinetic energy, and the character of the deep mean flow. The most realistic experiment compares to within a factor of two or better with observations of the amplitude of eddy kinetic energy and rms fluctuations of the thermocline and sea surface height. Abyssal eddy kinetic energy was smaller than observed. The mean flow is characterized by recirculations to the north and south of the Gulf Stream and a deep cyclonic gyre just east of the northern portion of the New England Seamount Chain, as found in the data.

Reprinted from: JOURNAL OF PHYSICAL OCEANOGRAPHY, Vol. 19, No. 6, June 1989
American Meteorological Society

A Limited-Area Model of the Gulf Stream: Design, Initial Experiments, and Model–Data Intercomparison*

J. DANA THOMPSON

Ocean Sensing and Prediction Division, Naval Ocean Research and Development Activity, Stennis Space Center, Mississippi

W. J. SCHMITZ, JR.

Woods Hole Oceanographic Institution, Woods Hole, Massachusetts

(Manuscript received 9 May 1988, in final form 5 January 1989)

ABSTRACT

A primitive-equation, *n*-layer, eddy-resolving circulation model has been applied to the Gulf Stream System from Cape Hatteras to east of the Grand Banks (78°–45°W, 30°–48°N). Within the limitations of the model, realistic coastlines, bottom topography, and forcing functions have been used. A two-layer version of the model was driven by observed mean climatological wind forcing and mass transport prescribed at inflow. Outflow was determined by a radiation boundary condition and an integral constraint on the mass field in each layer. Specification of a Deep Western Boundary Current (DWBC) was included in some model runs.

Six numerical experiments, from a series of over fifty integrated to statistical equilibrium, were selected for detailed description and intercomparison with observations. The basic case consisted of a flat bottom regime driven by wind forcing only. Realistic inflow transport in the upper layer was then prescribed and two different outflow specifications at the eastern boundary were studied in experiments 2 and 3. Three additional experiments involved (4) adding bottom topography (including the New England Seamount Chain), (5) adding a DWBC to experiment 4 with 20 Sv (Sv = 10^6 m^3 s^{-1}) total transport, and (6) increasing the DWBC to 40 Sv. A brief discussion of the influence of parameter variations includes modifications of dissipation (lateral eddy diffusion and bottom friction) and stratification.

Results from the sequence of experiments suggest an important role for the DWBC in determining the mean path of the Gulf Stream and consequently the distribution of eddy kinetic energy, and the character of the deep mean flow. The most realistic experiment compares to within a factor of two or better with observations of the amplitude of eddy kinetic energy and rms fluctuations of the thermocline and sea surface height. Abyssal eddy kinetic energy was smaller than observed. The mean flow is characterized by recirculations to the north and south of the Gulf Stream and a deep cyclonic gyre just east of the northern portion of the New England Seamount Chain, as found in the data.

1. Introduction

The dynamics associated with instabilities of western boundary currents and the role of the resultant mesoscale eddies in understanding the ocean general circulation are important topics in modern oceanography. Recently, eddy-resolving models have become sufficiently realistic and the data sufficiently extensive so that modellers and observationalists have begun to compare their respective results, notably those relevant to the Gulf Stream System. In a series of studies (e.g., Schmitz and Holland 1982; Holland and Schmitz 1985; Schmitz and Holland 1986; henceforth designated SH82, HS85, and SH86, respectively) results from mostly rectangular-domain quasigeostrophic numerical models were compared with observations of time averages from the western North Atlantic and Pacific. In essence these papers addressed the question: Can an eddy-resolving ocean model simulate the observed distributions of ocean variability as measured, for example, by eddy kinetic energy amplitudes, mean flows, and distributions of the off-diagonal components of the horizontal Reynolds' stresses?

The eddy kinetic energy distributions in the midlatitude North Atlantic are now known in general outline. For example, Fig. 1a shows eddy kinetic energy (EKE) calculated from surface drifters (Richardson 1983). At the surface there is a small region of maximum kinetic energy greater than 2000 cm^2 s^{-2} (and perhaps greater than 3000 cm^2 s^{-2}) west of the New England Seamount Chain (NESC). These results are in rough agreement with estimates of EKE from altimetric measurements (GEOS-3) by Douglas et al.

* NORDA Contribution 323:058:88 and Woods Hole Oceanographic Institution Contribution No. 6817.

Corresponding author address: Dr. J. Dana Thompson, NORDA, Code 323, NSTL Station, MS 39529-5004.

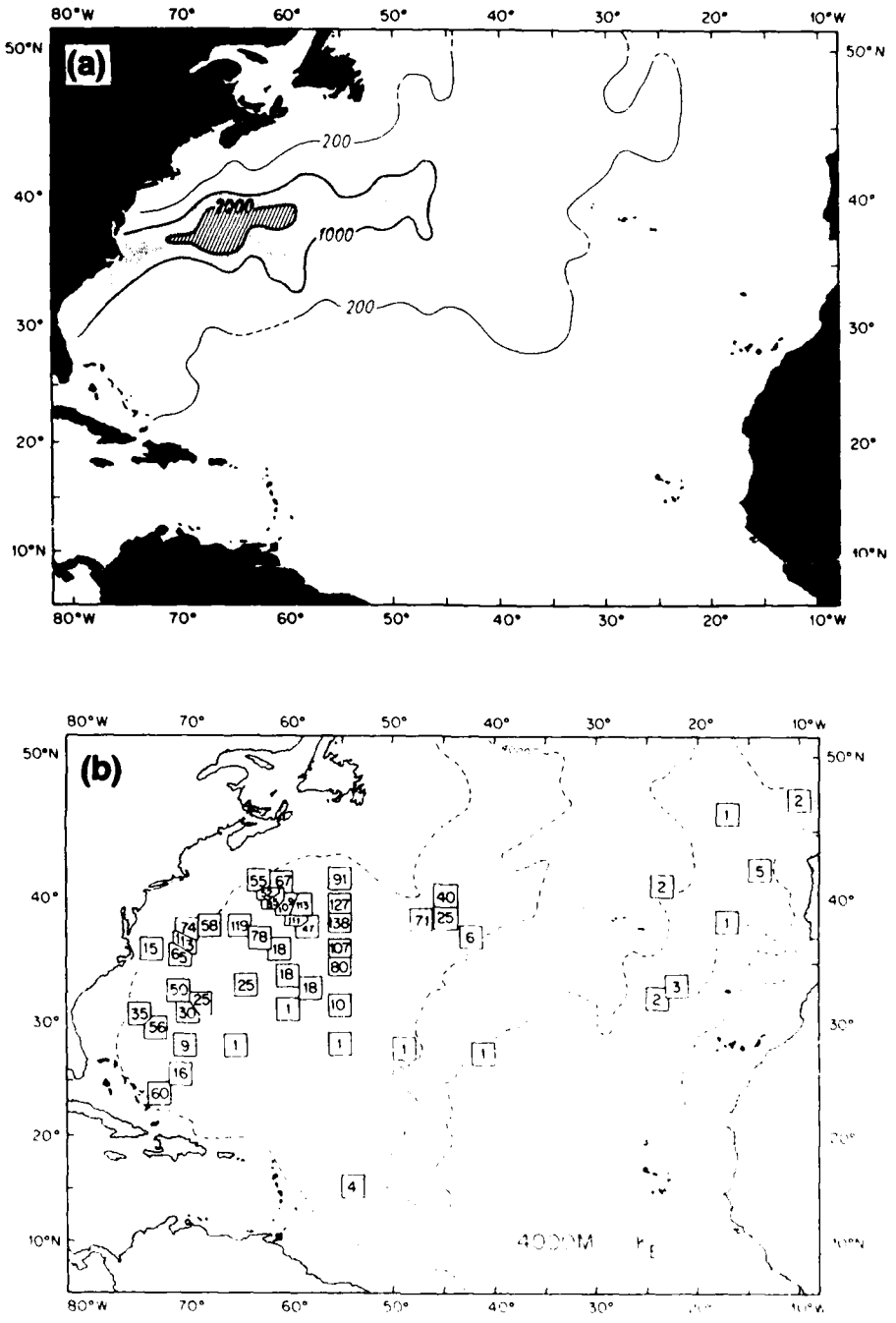

FIG. 1. (a) Eddy kinetic energy of the upper ocean (in $cm^2 s^{-2}$) determined from drifters (Richardson 1983). (b) Updated chart of the existing estimates of abyssal eddy kinetic energy ($cm^2 s^{-2}$) in the North Atlantic. (See also Schmitz 1984).

(1983), but are higher than those estimated from ship drift (Wyrtki et al. 1976). Figure 1b is an updated map of abyssal eddy kinetic energy estimates for the North Atlantic. Most of the data sources have been described in Schmitz (1984). The maximum of 140 $cm^2 s^{-2}$ in EKE east of the NESC at 55°W at the latitude of the mean Gulf Stream is notable, as is a two order of magnitude latitudinal decay into the interior of the subtropical gyre in both zonal and meridional directions. In addition to the information on EKE, a coherent picture of the deep mean flow in the western North Atlantic is beginning to emerge. For example, Fig. 1c is a map of long-term current meter measurements from Hogg et al. (1986). Also shown is the mean position of the 15°C isotherm at 200 m adapted from Fisher (1977). The DWBC flowing along the conti-

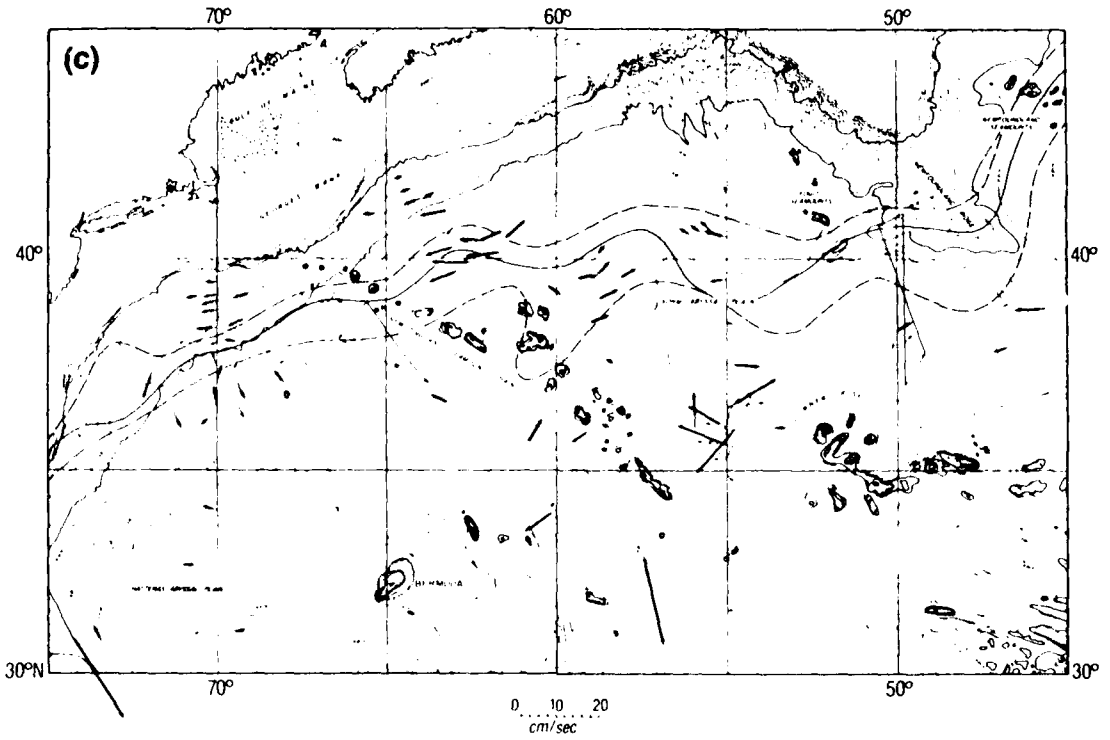

FIG. 1. (*Continued*) (c) Deep mean velocities from measurements compiled by Hogg et al. (1986). The thin portion of the arrow is an estimate of the uncertainty in the mean resulting from eddy noise. Also shown (solid thin line) is the mean position of the 15°C isotherm at 200 m adapted from Fisher (1977). The isotherm is between the dashed lines 50% of the time.

nental rise, an offshore "northern recirculating gyre," and a strong westward flow north of about 40°N just east of the Seamount Chain with no counterpart at similar depths further to the west are all noted by Hogg et al. (1986). An anticyclonic circulation around the northeast extension of the Bermuda Rise centered near 35°N, 60°W was also identified in the data.

In general the early two-layer model solutions of SH82 possessed the basic property that the most energetic eddies were located near strong currents which, in turn, were fed by return circulations. However, the zonal scale for both the mean and the eddy flow were smaller than observed. The HS85 experiments demonstrated that increased vertical resolution, increased lateral friction, and introduction of a gentle bottom slope can improve the penetration scale of the model Gulf Stream by confining the input of wind energy to shallower upper layers and inhibiting instability processes. In the higher resolution (eight layer) experiments of SH86, zonal and vertical distributions of eddy kinetic energy near both the Kuroshio Extension and the Gulf Stream were in reasonable agreement with observations, though better for the North Pacific than the North Atlantic. However, mean zonal currents at some locations in the midlatitude jet were clearly higher than observed and the data-based surface KE distribution along the Gulf Stream and the model analogue were different in shape, possibly due to the New England Seamount Chain or topography in general. Model equivalent isotherm depth fluctuations were smaller than observed.

The selection of precise geographical locations at which to compare model and observations has not been straightforward since model geometry and wind forcing have been idealized. Until recently most of the modeling experiments have utilized quasigeostrophic dynamics in regular domains with idealized winds, with the mean path of the modeled Gulf Stream being entirely zonal, coincident with the zero curl line of the mean wind forcing. Comparison with actual wind fields in the North Atlantic suggests that, even with the uncertainties in the data, the Gulf Stream mean path is significantly different from the zero curl line of the mean annual wind and distinctively nonzonal. Also, a condition of the QG approximation is that bottom topography must be of small amplitude, no more than 10% of the fluid depth. Such a condition is inappropriate near the continental slope or within the New England Seamount Chain (NESC), where seamounts rise 3 km above the surrounding sea floor and come within 1 km of the sea surface. Furthermore, Harrison (1982) has shown that there can be no net vorticity input to the lower layer of a QG model via vortex stretching.

Thompson and Hurlburt (1982) and Hurlburt and Thompson (1984), henceforth referred to as TH82 and HT84, developed a primitive equation model of the Gulf Stream including large-amplitude bottom topography. In the HT84 study a rectangular model domain rotated 28 degrees counterclockwise from zonal extended from Cape Hatteras to the Grand Banks. The model domain was closed except for an inflow port at Cape Hatteras and an outflow port roughly at the mean position of the Gulf Stream as it passes south of the Grand Banks. In all of the experiments the flow of the Gulf Stream was confined to the upper layer of the model and did not directly impinge on the topography. Flow in the lower layer was driven from above by pressure fluctuations associated with the active upper ocean. The model NESC had a substantial influence on the Gulf Stream variability and mean path. Results from the reduced-gravity (equivalent barotropic) model were unrealistic, with length scales for rings and meanders too large by a factor of two. Addition of the barotropic mode and the possibility for baroclinic instability yielded a more realistic GS. Warm core ring generation was enhanced by the NESC, with prolific generation occurring immediately upstream of the NESC with a frequency of about 2 yr^{-1}. When compared to the flat bottom experiment, the NESC increased both baroclinic and barotropic instabilities as measured by the rate of transfer of mean potential to eddy potential energy and mean kinetic to eddy kinetic energy.

Maximum EKE in the large seamount experiment exceeded 2000 $cm^2 s^{-2}$ in the upper layer and 130 $cm^2 s^{-2}$ in the lower layer. Maximum sea height variability greater than 35 cm was found in the large amplitude seamount experiment, comparable to that observed by Douglas et al. (1983). These values are comparable to observations but location of the abyssal maximum was upstream of the seamounts, unlike the observations, and the flow east of the NESC was generally much too weak. An unresolved question in HT84 was the influence of the outflow boundary condition on the Gulf Stream mean path and energetics. Because the outflow was confined to a narrow port at approximately the latitude of the mean Gulf Stream it was possible that the mean path and the meanders of the Stream (and thus KE east of the NESC) were artificially constrained.

Adamec (1988) examined the effects of seamounts in a two-mode quasigeostrophic model and found that seamounts deflected the average model jet southward and induced a standing wave downstream. Additional vertical modes enhanced the baroclinic instability mechanism and reduced the eastward penetration of the jet. However, in contrast to HT84, the seamounts in the quasigeostrophic model had little effect on the distribution and magnitude of the eddy kinetic energy at the surface.

This paper is a logical extension of HT84, SH82, and HS85. Our purpose is to describe the experimental design and some results from a new primitive-equation regional model of the Gulf Stream including realistic geometry, bottom topography, and wind forcing. The model results are unique in that they represent statistically-equilibrated, eddy-resolving integrations of an open ocean region in an irregular domain. Although analysis and experimentation are ongoing, we report our initial efforts in this paper as follows. Section 2 describes the model domain, forcing, parameters, and inflow and outflow boundary specifications. Section 3 provides results from six experiments from a series of over fifty and compares model results with observations, focusing on areas of significant agreement and disagreement. One basic experiment serves as a benchmark about which bottom topography, a deep western boundary current, and modifications to the extent of the open outflow boundary condition are added. In section 4 we summarize our results, identify deficiencies in our approach, and suggest some future work. Finally, appendix B describes the numerical design and the open boundary conditions in some detail.

2. Experimental design

The HT84 Gulf Stream model was adapted from an earlier rectangular-domain primitive-equation formulation for the Gulf of Mexico by Hurlburt and Thompson (1980, hereafter HT80). Wallcraft and Thompson (1984) extended the model to include irregular coastlines, yielding the first eddy-resolving primitive-equation ocean model with realistic geometry, bottom topography and open boundary conditions capable of multiyear integrations to statistical equilibrium. Benchmark experiments using that model have been described by Thompson (1986) and by Hurlburt (1984).

Differences between the present model and Hurlburt and Thompson (1980) are described in appendix B. The model domain is shown in Fig. 2. Inflow and outflow specifications are described in section 3. Since a focus of this study is the influence of the DWBC on the Gulf Stream, we have modeled it via a specified transport in the deep layer centered along the 3000 m isobath of the continental slope in the northeast portion of the model with outflow along the southern boundary. Although only two-layer results will be reported here, the model has been formulated for arbitrary vertical resolution and three-layer experiments are underway. As is usual with adiabatic models with a Lagrangian vertical coordinate, topography is confined to the deepest layer of the system, and ventilation of the model thermocline is not permitted. If the upper layer thins to zero thickness the experiment must be terminated. It is possible to prevent such behavior and continue integrations, even in an adiabatic model, by employing techniques in shock wave modeling such as the Flux Corrected Transport Method (Boris and Book

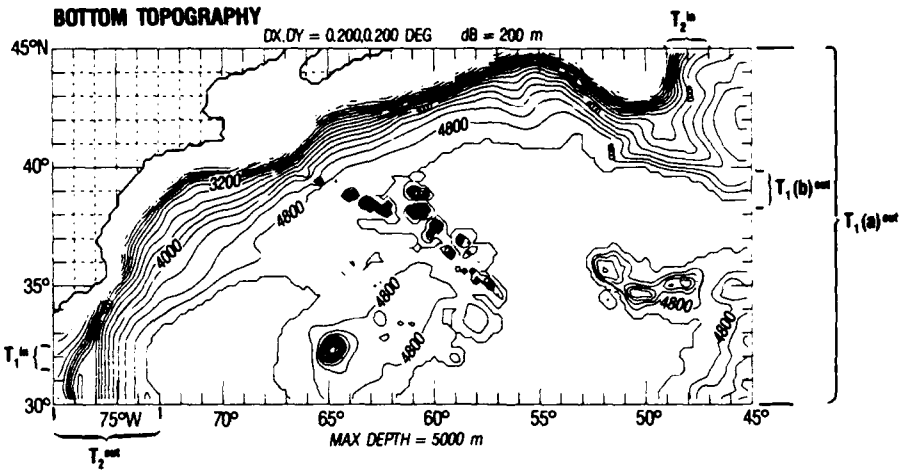

FIG. 2. Model domain for the limited-area Gulf Stream model. Bottom depths are shown with a 200 meter contour interval. Inflow (T_i^{in}) and outflow (T_i^{out}) location for upper ($i = 1$) and lower ($i = 2$) layer transports are also noted.

1973). The method has been applied by Bogue et al. (1986) for the problem of thermocline outcropping of the Gulf Stream but we have sidestepped the problem in these experiments by choosing a sufficiently thick upper layer at the initial time to avoid thermocline surfacing.

For the experiments with bottom topography the original SYNBAPS bathymetric data base (Van Wyckhouse 1979) was mapped to a 0.2 degree model grid. The model lateral boundary was taken to be located at the 200 m contour. Except at the ports the boundaries are rigid and the no-slip condition was imposed. A five-point smoother was applied twice to the full topography to damp high spatial variability and the result scaled such that the shallowest topography in the basin is at 1500 m (see Fig. 2).

Model parameters are provided in Table 1 and a summary of the numerical experiments are listed in Table 2. While it is not our purpose to conduct an exploration of parameter space in this paper, it is important to mention some of the model's sensitivities to parameter variations. First, the value of the density contrast between layers is based on the vertical density variation for a rather arbitrary mean density profile near the "center of the recirculation gyre." If the density contrast is reduced the thermocline will eventually surface. If the density contrast is increased the thermocline fluctuations become too small and unrealistic. With respect to horizontal eddy viscosity for the Laplacian lateral friction, we have chosen the lowest value (100 m s^{-2}) which was numerically stable for the 0.2 degree horizontal resolution. The maximum grid interval Reynolds number for this choice of lateral friction is around 150. For the quadratic bottom friction we have used a stress coefficient (C_b) ranging from zero to 2×10^{-3}. In the flat bottom experiments it is necessary to include bottom friction to insure statistical equilibrium at realistic energy levels. Otherwise baroclinic instabilities transfer energy to the deep water at a rate which cannot be dissipated via lateral friction or exported from the domain. However, in the experiments with bottom topography, baroclinic instability processes tend to be inhibited and energy transfer to the deep water is slowed. Consequently bottom friction is not necessary for statistical equilibrium in these experiments. Experiments 5a ($C_b = 0$) and 5b ($C_b = 2 \times 10^{-3}$) illustrate this model sensitivity.

TABLE 1. Model parameters.

A	10^6 cm^2 s^{-1}
g	980 cm s^{-2}
g'	2 cm s^{-2}
H_1	1000 m
H_2	4000 m
$\Delta x, \Delta y$	0.2°
Δt	60 min
C_b	0 and 2×10^{-3}

3. Experimental results

The extent to which local wind forcing alone determines the mean path, strength of the Stream and its recirculation, and the intensity of the eddy activity in the absence of forced inflow is the focus of Experiment 1. The model was driven from rest with mean annual wind forcing derived from 12-hourly FNOC surface (19 m) analyses from 1979 to 1984. The resulting wind stress curl field is shown in Fig. 3a. The zero-curl contour is nonzonal and the wind curl distribution is similar to that derived by Hellerman and Rosenstein (1983).

TABLE 2. Model experiments.

Experiment	C_b	Transport (Sv)* (Layer 1/Layer 2)	Topography	Port forcing
1	2×10^{-3}	0/0; wind forced	No	closed boundaries
2	2×10^{-3}	50/0	No	narrow outflow
3	2×10^{-3}	50/0	No	wide outflow
4	0	50/0	Yes	wide outflow
5a	0	50/20	Yes	wide outflow
5b	2×10^{-3}	50/20	Yes	wide outflow
6	0	50/40	Yes	wide outflow

Transport profiles on inflow are parabolic.
Lower layer transport represents the Deep Western Boundary Current flowing along the continental slope.
* Transport on Inflow = Transport on Outflow for each layer.

Figure 3b shows the synoptic sea surface height (SSH) for Experiment 1 following spinup to statistical equilibrium (requiring about 6 years). To first order this pattern is also the pattern of model thermocline anomaly, with a 10 cm change in SSH equivalent to about a 50 m change in thermocline anomaly. There is a weak Gulf Stream [about 20 Sv ($Sv \equiv 10^6\ m^3\ s^{-1}$) on average, consistent with the mean wind curl] extending from Cape Hatteras northeastward and intense recirculations north of the stream near the coast and in the southwest corner of the domain. Instantaneous penetration of the Stream into the domain only extends to about 65°W. Eddy activity is evident from the SSH field in the weak meandering of the Stream and in the cyclonic eddy centered at about 34°N, 73°W. The eddy field is much more clearly shown in the subthermocline pressure field (Fig. 3c). The basin is nearly filled with eddies. Although a large barotropic Rossby wave response is excited during the early spinup, the deep eddy field shown here in year 9 is energized via instabilities of the Gulf Stream and associated wave radiation.

The mean SSH is shown in Fig. 4a. The tight recirculation to the south of Cape Hatteras is due, in part, to the influence of the rigid wall at 30°N. An important aspect of the mean flow is the cyclonic recirculation to the north of the Stream and the southward flow along the coast between Cape Hatteras and Cape Cod. As will be shown later, a critical determinant for separation of the Gulf Stream is the intensity of the southward flow in this region, both at the surface and below the thermocline (in the DWBC).

Maps of the eddy kinetic energy (EKE) above and below the thermocline (upper and lower layers) for Experiment 1 are shown in Fig. 4b and 4c. The upper layer EKE is very weak, about 10% of the observed surface EKE (Richardson 1983) and fails to penetrate east of 60°W. (Note the model "surface" values are really a layer average over 1000 m in the mean and thus cannot be directly compared with surface estimates from drifters). The largest surface EKE values are in the recirculation zone where the mean flow is southwestward. Deep EKE is also much weaker than observed (Schmitz 1984), having maximum values less than 11 $cm^2\ s^{-2}$ (compared to 140 $cm^2\ s^{-2}$ from observations), and is confined to west of 60°W.

Experiment 2 utilizes the addition of the inflow transport south of Cape Hatteras. The details of the inflow and outflow boundary conditions are in appendix B. The model supports specification of either transport or current profile plus the inflow angle and requires conservation of mass in the domain at all times. We specify a steady inflow transport and cross-stream profile based on data from Richardson et al. (1969). Total upper layer inflow transport is 50 Sv, distributed over a 100 km wide inflow with a parabolic cross-stream profile, and an inflow angle of 28 degrees. The model is spun up with an e-folding time of one year (see appendix B). Surprisingly, the model was not very sensitive to inflow angle (although more experiments are necessary to understand inflow angle dependencies and sensitivities to time dependent inflow transports).

Two variations of the outflow condition were considered. The first, used in Experiment 2, prescribed a narrow (100 km wide) outflow boundary port centered at 39°N, approximately the location of the climatological mean Gulf Stream at 45°W. This is similar to the approach used earlier in HT84. The second condition allows the entire eastern boundary in the upper layer to be open and is used in the remainder of the experiments. The requirements for mass balance and the possibility of a return circulation are discussed in appendix B.

Experiment 2 was integrated to statistical equilibrium as before. Figure 5a shows a snapshot of the sea surface height in model year 20. The meanders of the Stream, warm and cold rings, and the recirculation are evident. The maximum SSH variation is over 140 cm and the height change across the Stream is comparable to observation, about one meter. The mean SSH in Fig. 5b shows a standing wave for the Stream with a meander wavelength of approximately 600 km and maximum amplitude of about 150 km. Halliwell and Mooers (1983) found a standing meander of comparable wavelength downstream from Cape Hatteras us-

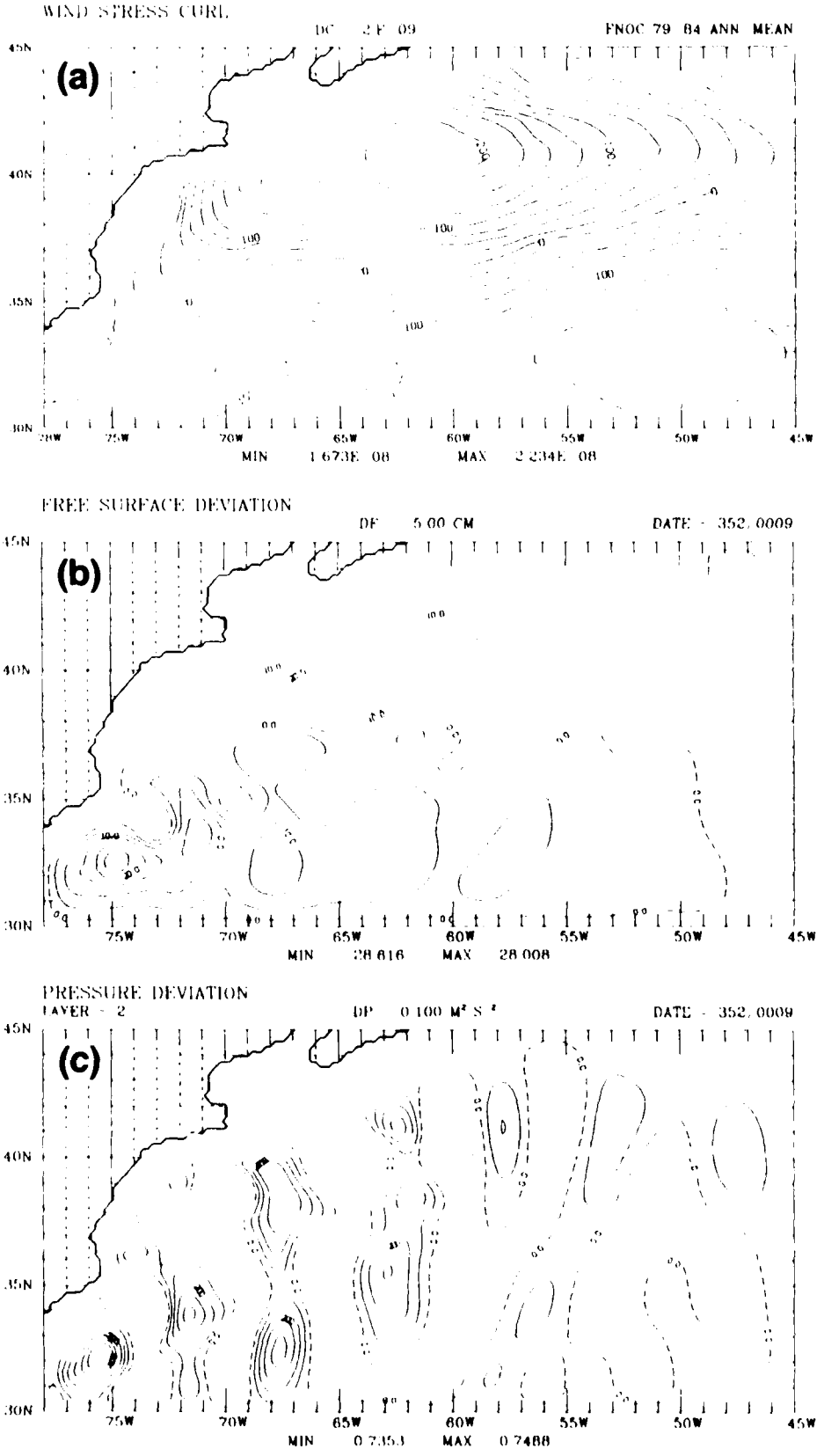

FIG. 3. (a) Mean annual wind stress curl from 12-hour FNOC analyses from 1979 to 1984. Contour interval is 2.0×10^{-9} dyn cm^{-3}. (b) Sea surface height anomaly (SSH) at year 9, day 352 for Experiment 1. Contour interval is 5 cm. (c) Density-normalized lower-layer pressure anomaly (PA2) at year 9, day 352 for Experiment 1. Contour interval is 0.1 m^2 s^{-2}.

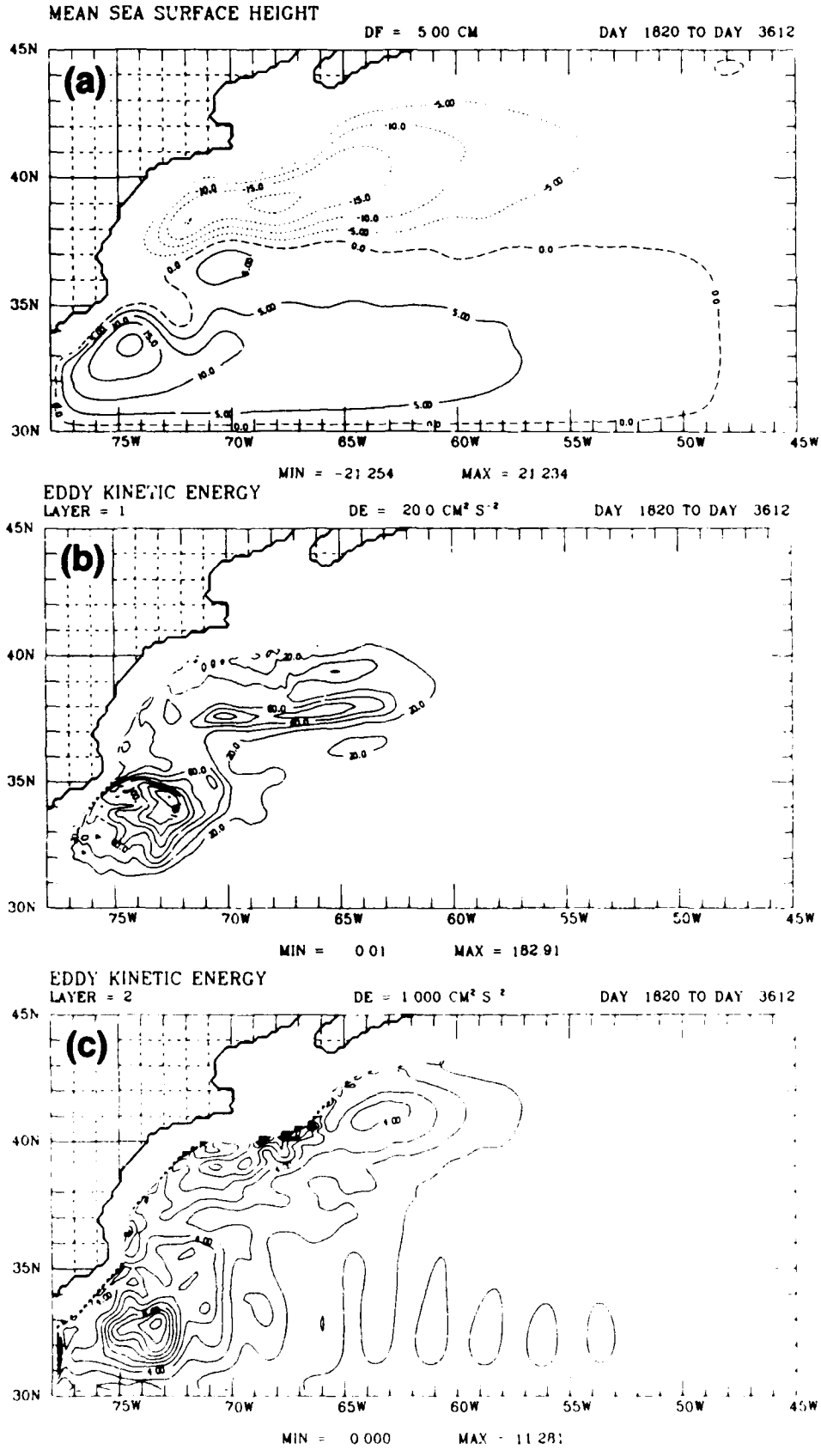

FIG. 4. (a) Mean SSH for Experiment 1 in statistical equilibrium. Contour interval is 5 cm. (b) Upper-layer eddy kinetic energy (EKE1). Contour interval is 20 $cm^2 s^{-2}$. (c) Lower-layer eddy kinetic energy (EKE2). Contour interval is 1.0 $cm s^{-2}$.

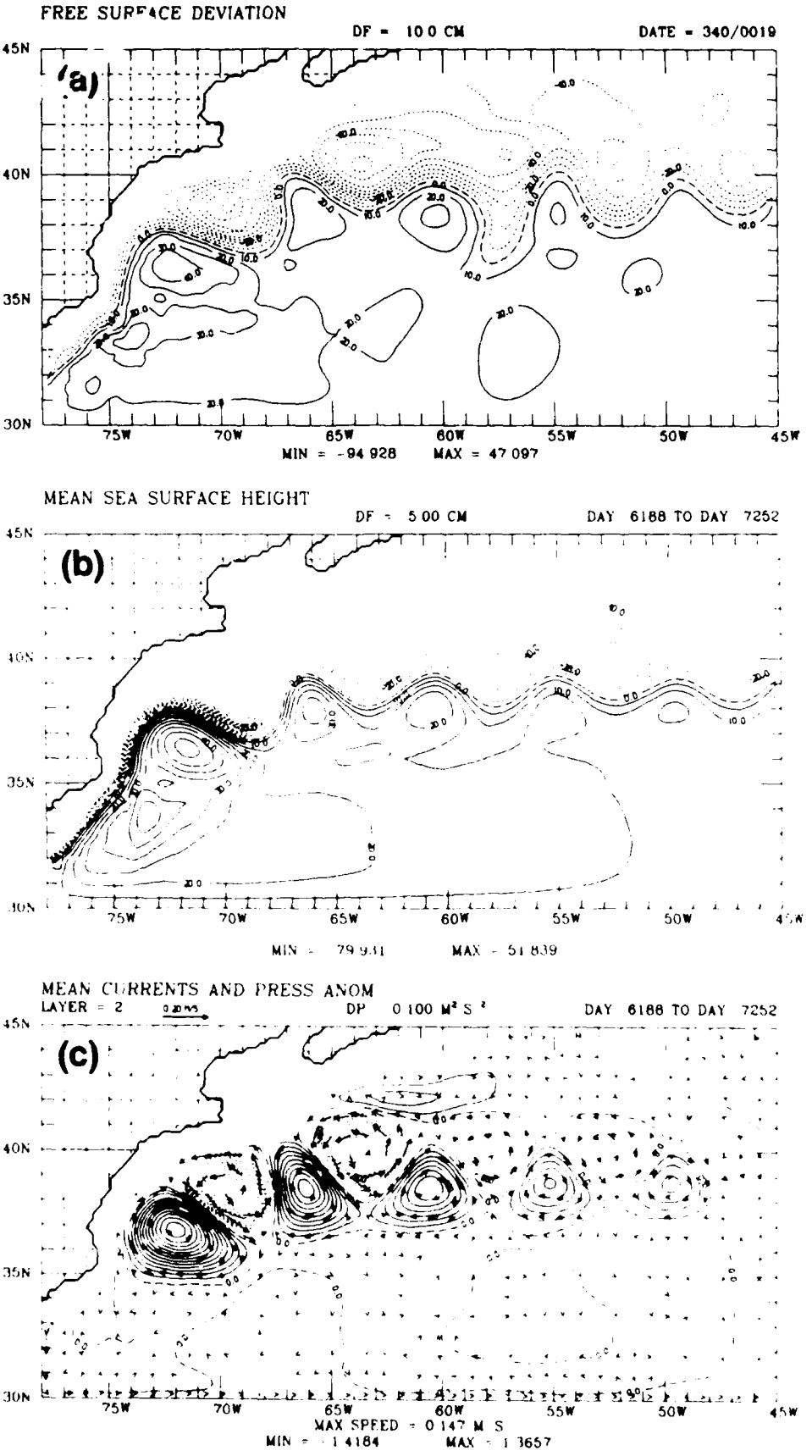

FIG. 5. Results from Experiment 2 for: (a) SSH at year 19, Day 340. Contour interval is 10 cm. (b) Mean SSH (5 cm contour interval). (c) Deep mean currents and mean PA2 (0.1 m s^{-2} contour interval).

ing Naval Oceanographic Office analyses of satellite infrared imagery from 1975 to 1978. As the Stream approaches the outflow boundary the meander amplitude must decrease to almost zero. The deep mean flow is depicted via the mean pressure (Fig. 5c), with stationary closed circulations in phase with the standing waves in the mean Gulf Stream. There is a strong barotropic component to the circulation in these regions. Recirculation zones to the north and south of the Stream are clearly depicted.

Experiment 3 is identical to Experiment 2 except that the entire eastern boundary is opened. Both the instantaneous (Fig. 6a) and the mean (Fig. 6b) path of the model Gulf Stream are well north of those from the narrow outflow experiment. The amplitude of the (standing) meanders of the mean Stream in Experiment 3 are smaller in the eastern half of the domain than for Experiment 2. Likewise, below the thermocline the standing eddies are largely confined to the western part of the domain (Fig. 6c).

The tendency for the model Gulf Stream to extend too far north is very clear. One explanation for this behavior is that the Stream is not sufficiently inertial to separate at Cape Hatteras. We have conducted several experiments in which we have increased the maximum current speed in the Stream by up to 50%, both by increasing upper layer transport and by using a thinner upper layer. The Stream did not separate significantly farther south in these experiments. A large barotropic anticyclonic recirculation south of the Gulf Stream forms just downstream from Cape Hatteras in the mean flow, tending to help deflect the current north along the coast. This recirculation intensifies with increased Gulf Stream currents at inflow. Surprisingly, moving the southern boundary five degrees farther south did not significantly alter the tendency for overshoot to occur. Even when the lateral boundary was chosen be the actual coastline rather than the 200 m isobath, overshoot still occurred. While higher vertical resolution may resolve this problem, to our knowledge all "realistic" Gulf Stream models with higher vertical resolution share this tendency for overshoot. For example it is quite clear in the results of Cox (1985, Fig. 3b) in an 18-level, one-third degree integration of the GFDL model. As an aside, W. Holland (personal communication) finds that overshoot can be less severe with lower values of lateral eddy viscosity.

The deep eddy kinetic energy fields for experiments 2 and 3 are shown in Fig. 7a and 7b. The eddy kinetic energy levels are consistently lower in the narrow outflow experiment. Values near 60 $cm^2 s^{-2}$ occur in the wide outflow case but values less than half that are found in the narrow outflow case. These two experiments present us with a dilemma. On one hand, the mean path is overall better represented when we fix the outflow boundary as a narrow port, but the mean path is too far north when we open the entire domain. However, the deep eddy kinetic energy is more realistic in the wide outflow experiment. How might we resolve these dichotomous results?

Before answering this question we should inquire as to the influence of topography on the circulation. Experiment 4 is defined by the addition of the bottom topography to Experiment 3. Following spinup the model yields the mean SSH shown in Fig. 8a. The GS mean path is quite unrealistic, hugging the coast much too far north before turning eastward. The deep mean pressure in Fig. 8b exhibits length scales comparable to those of the topography. The mean anticyclonic circulation around Bermuda and southwest of the southern portion of the NESC are particularly striking, as is the mean anticyclonic and two cyclonic gyres east of the NESC underneath the Gulf Stream. The deep EKE is also very different from that from the flat bottom experiments (see Fig. 12a). With the addition of bottom topography the maximum deep EKE increases to over 80 $cm^2 s^{-1}$ and is largely confined west of the NESC.

One approach to the problem of separation of the Gulf Stream might be to include an additional vorticity source, such as a deep southward-flowing current. Such a current was postulated by Stommel (1958) as a means of supplying cold water from the north to feed the slow upwelling in the ocean interior and was first observed by Swallow and Worthington (1961). It has since been termed the Deep Western Boundary Current (Hogg 1983). Estimates of its strength have ranged from a few Sverdrups up to 40 Sv (Riser et al. 1978). Lai (1984) found that an L-shaped array of current meters along and across the Blake Escarpment yielded a DWBC with a mean transport of 24 Sv over a hundred day record. The core of the current was situated at about 2500 m, 10 km east of the break in the Escarpment. Hogg et al. (1986) report a transport of 20 Sv carried by the DWBC and the slope current at 70°W. Additionally, Mellor et al. (1982) found in a diagnostic calculation of the general circulation of the Atlantic a strong (25 Sv), southwestward flowing, nearly barotropic current along the continental slope in the North and Middle Atlantic Bight. Olbers et al. (1985), using a beta-spiral technique, have inferred a comparable southward flow at 2000 m along the continental slope of the northwestern Atlantic. Mellor (personal communication) has found this slope current to be critical for separation of the Gulf Stream off Cape Hatteras in a sigma-coordinate primitive equation model.

In the model we have imposed a DWBC as a deep inflow along the eastern side of the northern boundary via a 100 km wide stream centered near the 3000 m isobath with a parabolic transport distribution. Figure 9 shows the spinup process via the time series of potential and kinetic energies averaged over the domain. The scale for potential energy is fivefold that for kinetic energy. Note the time scale required to reach statistical

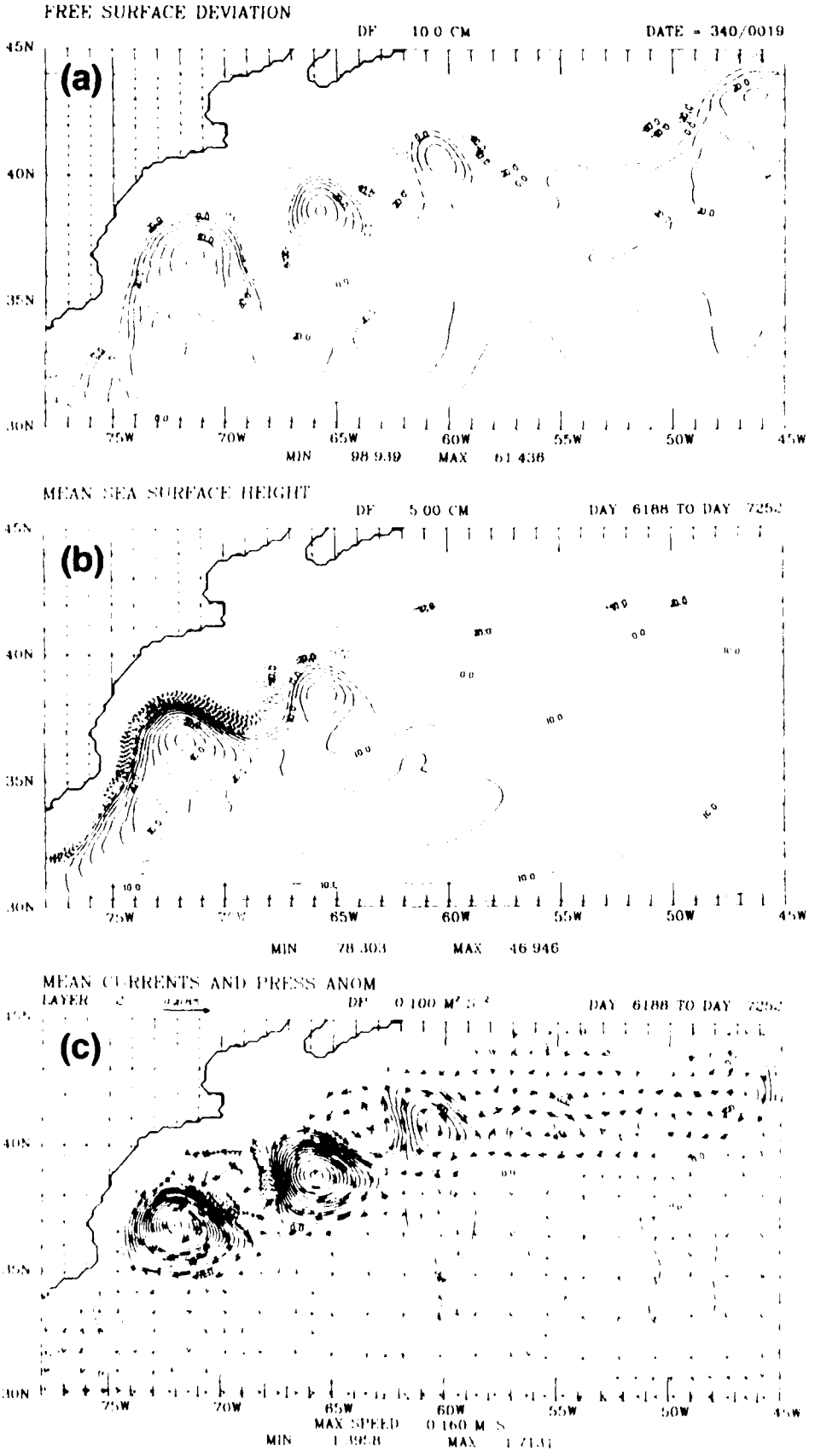

FIG. 6. As in Fig. 5 but for Experiment 3, Day 353 in (a).

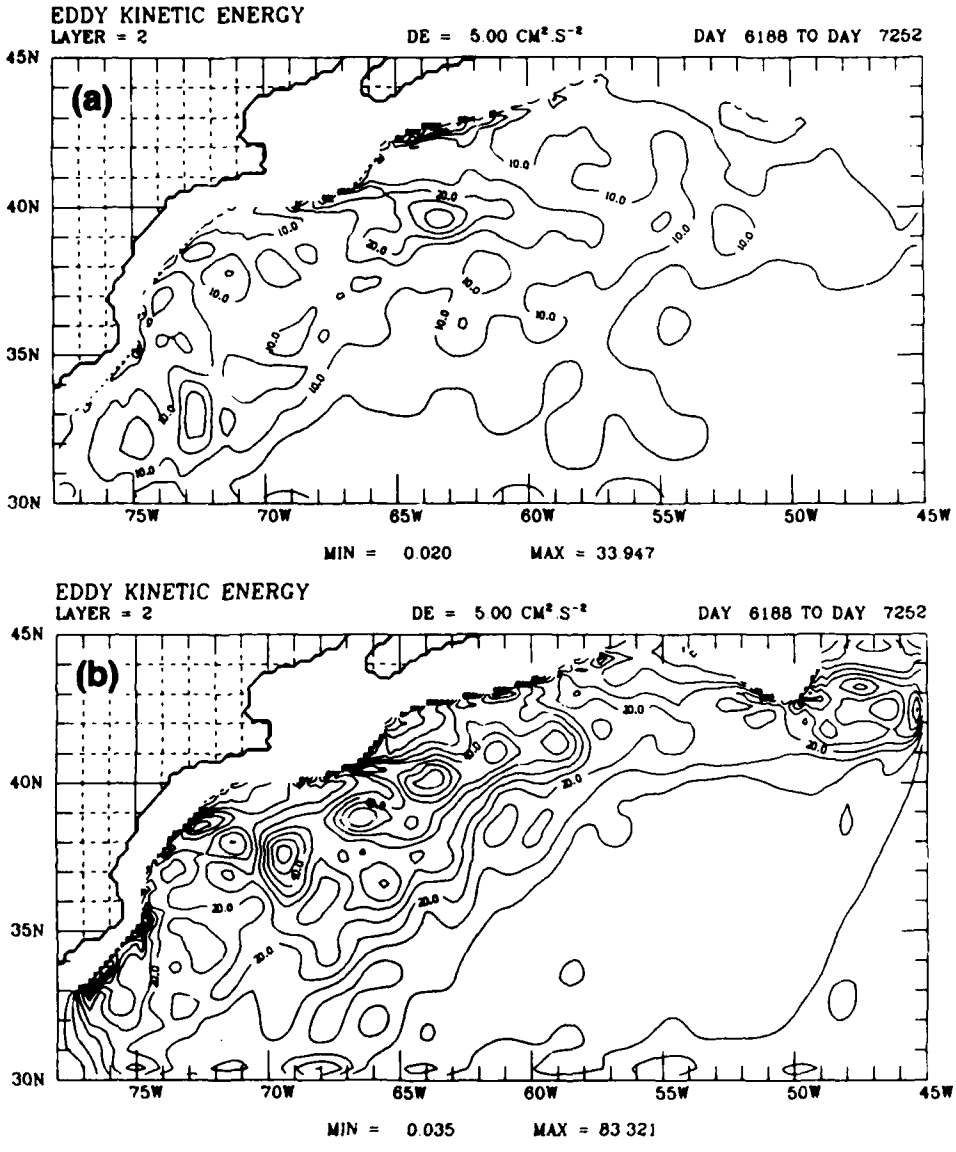

FIG. 7. (a) EKE2 for Experiment 2. (b) EKE2 for Experiment 3. Contour interval is 5 $cm^2 s^{-2}$.

equilibrium is 8–10 years and that significant energetic fluctuations have time scales of several months to several years after equilibrium is attained.

Figure 10a shows the mean sea surface for Experiment 5 (DWBC = 20 Sv) after statistical equilibrium is reached. Notice that the mean Stream has separated from the coast at a lower latitude and that the return circulation fills the region to the south of the Stream in the model interior.

The deep mean pressure and the deep mean velocity vectors are shown in Fig. 10b. The mean velocities readily indicate the location of the DWBC along the continental slope and tend to follow the contours of f/h. The deep pressure pattern is somewhat similar to that without the DWBC but is considerably strengthened. With the exception of eddy energy estimates, the most extensive data set which can be compared in the western North Atlantic over long time periods is the deep mean flow. Hogg (1983) compiled all of the long-term deep current meter measurements in this region. He has recently updated that map (Hogg et al. 1986) as shown in Fig. 1c. While there are numerous detailed comparisons to be made we will focus on four specific areas: 1) the recirculation zone near the region of the HEBBLE experiment at 41°N, 63°W, 2) the foot of the continental rise near 68°W, 37°N, 3) the region of the "northern recirculating gyre" north of 40°N along 55°W, and 4) the flow around isolated seamounts such as Corner Rise.

Hogg (1983) identified two separate deep flow regimes, the classical DWBC flowing along the continental rise and a second system of recirculating classical slope water gyres farther offshore. However these regimes are not always distinct. For example, Hogg

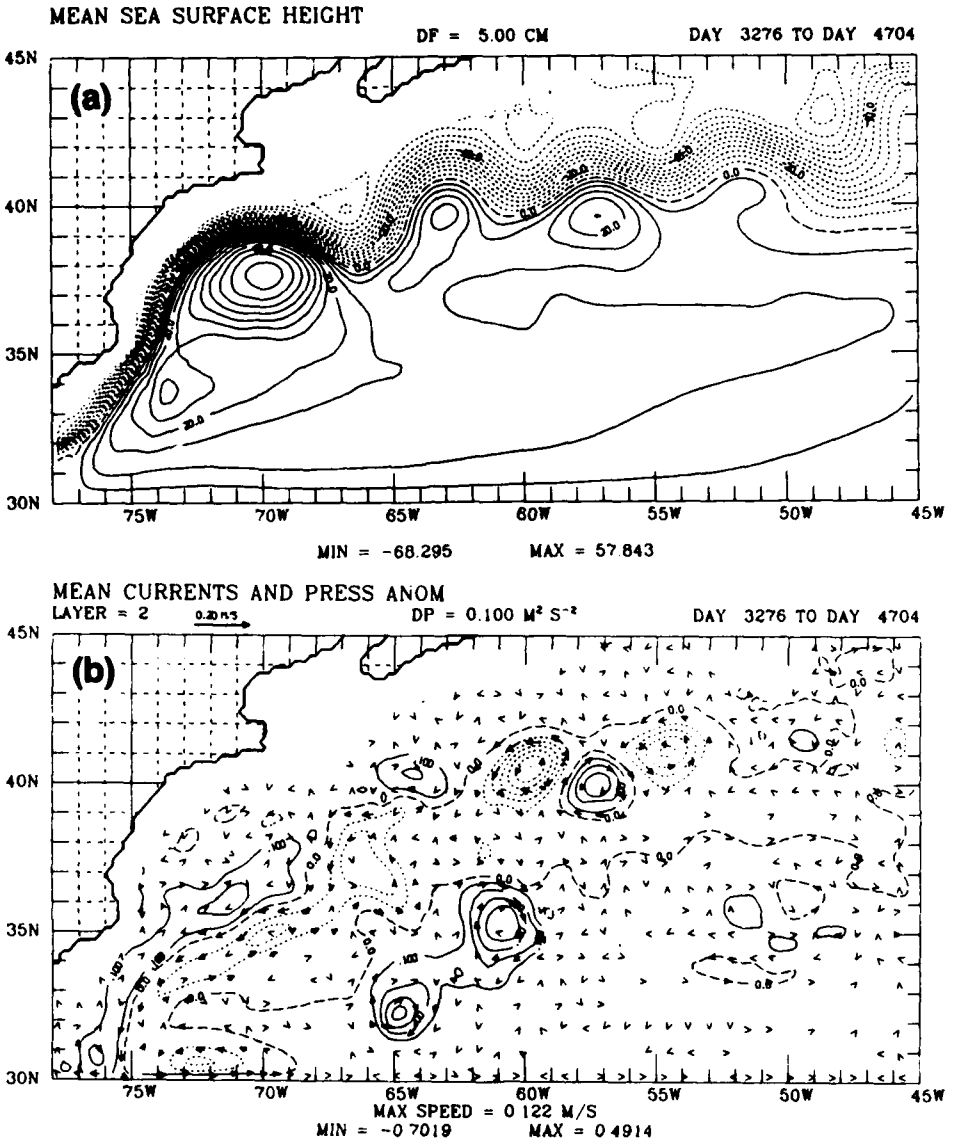

FIG. 8. Experiment 4 (a) mean SSH. Contour interval is 5 cm. (b) Deep mean currents and mean PA2. Contour interval is 0.1 m s^{-2}.

(1983) and Hogg et al. (1986) found that the Wunsch and Grant (1982) circulation scheme, deduced from an inversion of hydrographic data, could not easily account for the HEBBLE data. It suggested as much as 40 Sv flowing along the 4000 m isobath near 63°W was not evident at 70°W. Hogg surmised that there was a decoupling between the two currents such that a recirculation existed in the deep flow in the HEBBLE area. Such a recirculation is very much evident in the deep mean flow from the model with the magnitude of the recirculation being about 35 Sv. This circulation is indeed decoupled from that near 70°W. In fact, a separate "near-mesoscale" recirculation zone exists to the southwest along the foot of the continental rise centered near 37°N, 68°W and may explain the Rise Array data. In particular, the shoreward flow at the 4800 m isobath near 37°N, 68°W is found in the observations. The model results clearly point toward the need for additional measurements to determine if a closed gyre exists.

In Hogg's 1983 schematic the current meter array near 40°N, 59°W was not available and Hogg suggested the deep flow in this region was westward. However, Fig. 1c (from 1986) clearly shows that the currents in this area are flowing toward the northeast. The model results show that the eastern side of the "Hebble recirculation" is also the western side of a small anticyclonic gyre which splits what Hogg termed the "northern recirculating gyre" into two separate closed cyclonic gyres. The anticyclonic circulation is reminiscent of that suggested by Schmitz (1980) [and by Richardson (1981) from one degree box-averaged temperature data

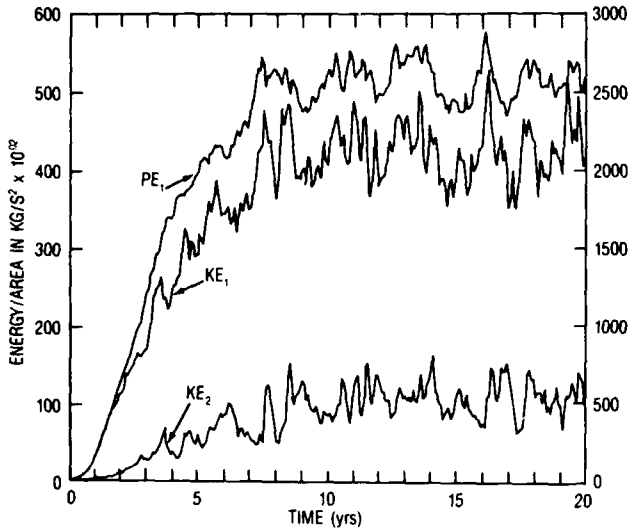

FIG. 9. Time series of basin-averaged potential energy per unit area due to thermocline (model interface) fluctuations and upper and lower layer kinetic energy per unit area in units of kg s^{-2}. Scale on the left refers to kinetic energy while scale on the right refers to potential energy.

at 450 m], although the model gyre is farther north and west of that indicated in the observations. The eastern cyclonic gyre centered near 41°N, 55°W is dynamically similar to that outlined by Hogg and Stommel (1985) in that this deep gyre is nearly potential vorticity conserving.

To illustrate the influence of the DWBC on the Gulf Stream we have plotted in Fig. 11 the observed mean path of the 15°C isotherm at 200 m (adapted from Fisher 1977) versus the axis of the mean current above the thermocline for three experiments differing only in the intensity of the lower layer flow: No DWBC, a 20 Sv DWBC, and a 40 Sv DWBC. As we increase the DWBC magnitude the mean path of the model jet is shifted further south. In fact the separation latitude is shifted by 150 km over the range of transports. As the transport of the DWBC is increased, the model Gulf Stream path is shifted southward, agreeing best with observations at a transport of 20 Sv. West of the seamounts, as the DWBC intensifies, the standing meander amplitude and the recirculation transport tend to decrease. Near Cape Hatteras, there is an overshoot of all modeled paths relative to observation, decreasing in amplitude and zonal scale with increasing transport. Note that the mean current is mainly north of the NESC in Expts. 4 and 5 but through them in Experiment 6. Interestingly, Auer (1987) has found a statistically significant northward shift in the Gulf Stream over five years from 1980 to 1985 of more than half a degree latitude. He has no explanation for the shift.

What are the dynamics which allow the DWBC to influence the mean path of the Gulf Stream? For the two-layer system they are very similar to those discussed in HT80 to explain how deep southward flow along the west Florida shelf could prevent northward penetration of the Loop current. HT84 also used these dynamics to show how fluctuations in the deep flow, rectified by the NESC, could alter the mean path of the Gulf Stream. From simple kinematics, the continuity equation for the upper layer can be written as

$$h_{1t} + h_1 \nabla \cdot \mathbf{v}_1 + \mathbf{v}_1 \cdot \nabla h_1 = 0. \qquad (3.1)$$

The third term on the left hand side of (3.1) represents nonlinear advection of upper layer thickness by a component of the upper layer flow. For nearly geostrophic flow,

$$\mathbf{v}_1 \cdot \nabla h_1 \approx \mathbf{v}_{1g} \cdot \nabla h_1 = \mathbf{v}_{2g} \cdot \nabla h_1 = J(\eta_1, \eta_2), \qquad (3.2)$$

where $\mathbf{v}_{ig}$ is the geostrophic velocity component in layer i, J is the Jacobian operator, η_1 is the deviation of the free surface from its initial value, and η_2 is the deviation of the interface between layers from its initial value. The term can be large when a strongly tilted thermocline (the interface in the Gulf Stream) intersects an intense deep flow (the DWBC) at a large angle. Physically it represents the interaction of a barotropic current and baroclinic current. Thus the barotropic component of the DWBC can advect the Gulf Stream at the point of intersection near the continental slope. For example, in Fig. 11 let the 0 DWBC curve represent the steady state position of the Gulf Stream. If we increase the DWBC transport to 20 Sv, say, nearly geostrophic deep flow moves southward closely following f/h contours (dominated by bottom topography nearly everywhere). Eventually the DWBC flows underneath the Gulf Stream. In Eq. (3.1) the initial steady state balance (with $h_{1t} = 0$) is altered such that, in the region of intersection of the Gulf Stream and the DWBC, $\mathbf{v}_1 \cdot \nabla h_1 \approx v_{2g} h_{1y} > 0$, since $v_{2g} < 0$ and $h_{1y} < 0$. Thus $h_{1t} < 0$ and the upper layer thickness decreases locally. As the layer thins, potential vorticity is conserved via the flow gaining anticyclonic relative vorticity and/or leaving the coast at a more southerly latitude, in effect shifting the Gulf Stream southward along the continental slope, as indicated in the 20 Sv (dashed-dot) curve of Fig. 11.

The significant influence of the DWBC on the Gulf Stream path clearly extends into the model interior. This change in the interior has radical consequences for the deep eddy field as well. In Fig. 12 we have plotted the deep eddy kinetic energy for the 0-, 20-, 40-Sv DWBC experiments (4, 5a, 6 respectively). In the case with no DWBC (Fig. 12a) the deep EKE is largely confined to a region west of the NESC with maximum values less than 80 $cm^2\ s^{-2}$. The NESC is also evident in the EKE contour pattern. In Fig. 12b we have plotted the EKE for the 20-Sv experiment. The distribution of EKE is more equally distributed east and west of the NESC with maximum values near 50 $cm^2\ s^{-1}$ to the east and 90 $cm^2\ s^{-2}$ to the west. For the 40-Sv DWBC case the EKE field is almost entirely shifted to east of the NESC with maximum values near 100 $cm^2\ s^{-2}$.

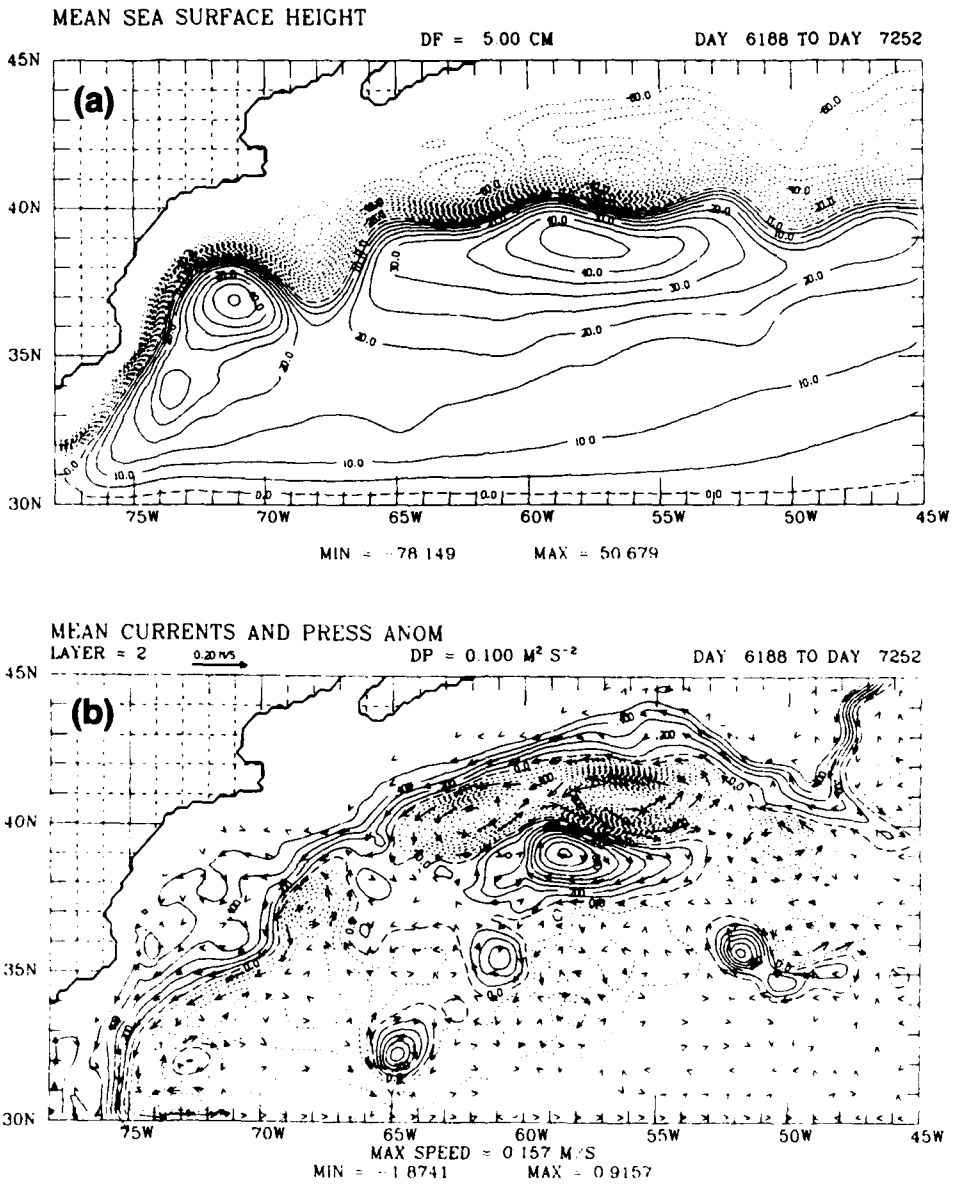

FIG. 10. As in Fig. 8 but for Experiment 5a.

These three experiments demonstrate that increasing the DWBC shifts the EKE distribution further eastward and toward higher amplitude as the mean path of the Gulf Stream shifts southward.

As we have noted earlier, an extensive comparison of long-term statistics for models and observations was conducted by HS86, primarily for deep EKE in the western North Atlantic and Pacific. This type of model/data intercomparison will continue to be a key test for any ocean model designed to simulate and explain the dynamics of midlatitude western boundary currents and eddies. Figure 1b shows a new updated map of deep eddy kinetic energy in the western North Atlantic. This is to be compared with the contour maps of deep EKE provided for Experiments 4, 5 and 6 in Fig. 12a–c, respectively. As mentioned earlier, as the DWBC transport increases the area of high deep EKE shifts to the east. For no DWBC the maximum value of about 85 $cm^2 s^{-2}$ is located near 37°N, 67°W, west of the seamounts, and is comparable to the observed values. Note also that large values also occur near the northern end of the NESC but confined to a very small area. Some indication of this same small scale distribution is shown in Fig. 1b as well, with values of 119 $cm^2 s^{-2}$ observed in a comparable location to that in the model. Near the model boundary there are also narrow maxima in EKE due to topographic waves. East of the NESC there are no values in excess of 40 $cm^2 s^{-2}$ for Experiment 4. When the DWBC is increased to 20 Sv in Experiment 6 the deep EKE field exhibits maxima to the east and west of the seamounts, with those to the west near 68.5°W being as large as 90 $cm^2 s^{-2}$ and

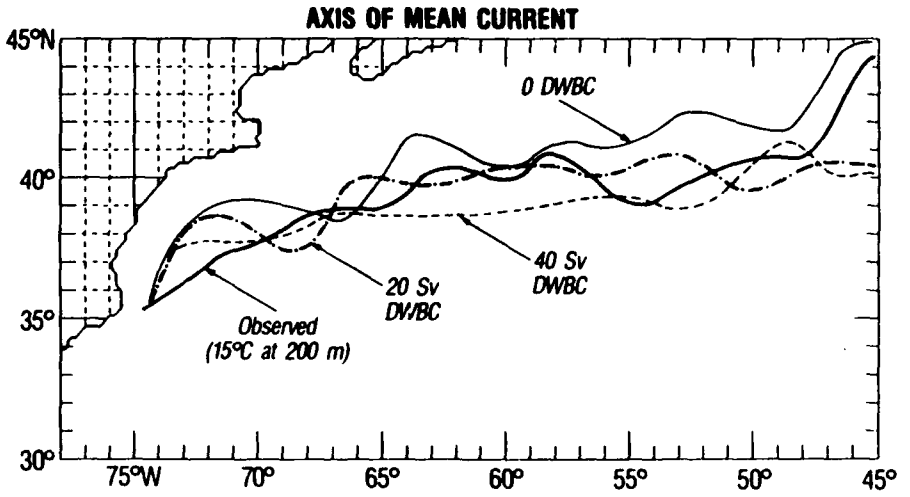

FIG. 11. Paths of the mean Gulf Stream. Axes of the upper layer current maximum for the long term mean for Experiments 4, 5a, and 6 and an estimate of the mean path of the Gulf Stream as indicated by the mean location of the 15°C. Isotherm at 200 m from Fisher (1977).

those to the east near 55°W not exceeding 50 $cm^2 s^{-2}$. Finally, for Experiment 6 with 40 Sv for the DWBC the eastward shift of the EKE field is nearly complete, having maximum values greater than 100 $cm^2 s^{-2}$ near 39°N, 53°W. This intercomparison of deep EKE suggests that the model amplitudes are too small by roughly a factor of two in comparison with the observations. All else being the same, time-dependent fluctuations in the inflow transport (or angle) and the wind driving should both act to increase deep EKE. While fluctuations in direct wind driving are unlikely to contribute significantly to abyssal EKE (Niiler and Koblinsky 1985), fluctuations in volume transport on seasonal to interannual time scales near Cape Hatteras may be much more critical. We do not suggest that the vertical and horizontal resolution, friction parameters, and stratification are less important in altering the amplitude and distribution of EKE in the model. In fact model sensitivity studies suggest that they may be more important than time-dependent forcing in this regard.

In Fig. 13a we show the rms SSH variability of Experiment 5a (20-Sv DWBC). The maximum value is about 40 cm to the west of the NESC chain. This corresponds well in amplitude with values determined by Marsh et al. (1984) based on SEASAT and GEOS-3 crossover data although location of the maximum is several degrees too far west in the model results. With the advent of GEOSAT we will have additional data on variability of the SSH in the Gulf Stream region to compare with these model results.

Figure 13b shows the associated field of thermocline variability (rms) for Experiment 5a. The magnitudes are comparable to those observed. For example, Fig. 13c compares the maximum rms variability from Experiment 5b at each longitude with Dantzler's (1977) calculation of the rms variability of the 15°C isotherm at 37° and 39°N. The magnitude of the rms thermocline variability is 10–20% higher in the experiment with bottom friction (5b) than without (5a). We are encouraged by two aspects of this comparison. First, the amplitudes of rms thermocline variability of the model are only slightly lower over the range of longitudes than observed. Since our model thermocline has a mean depth of 1000 m the variability of the 15°C isotherm is probably underestimated. This is offset by the fact that model variability was chosen not along constant latitudes lines but the latitude of maximum variability. Second, the model rms variability did not decrease significantly downstream to 45°N. at the outflow boundary. This suggests the boundary condition did not artificially constrain stream variability near the outflow.

The shallow EKE estimate from drifter data is shown in contour form in Fig. 1a (Schmitz et al. 1983; Richardson 1981). Model values are provided in Fig. 14 for the upper-layer EKE for Experiments 5a (a) and 5b (b). Note the upper-layer EKE levels to the east of the NESC are higher for the experiment with bottom friction although not very different to the west of the seamounts. A serious consideration with this comparison is that the mean thickness of the model upper layer is 1000 m while the surface drifter measurements are representative of the upper 100 meters or so. Based on estimates of vertical mean shear in the Gulf Stream region the model values are reasonable for the vertical average over 1000 m and are roughly half the surface EKE values (see SH86). The maximum value from observations is about 3000 $cm^2 s^{-2}$ located near 67°W while in the model the maximum value is about 2400 centered near the same longitude. In Fig. 14b the area covered by variability greater than 1000 $cm^2 s^{-2}$ is considerably greater than that from the model results. The downstream extent of the high variability in the model is comparable to that from the observations.

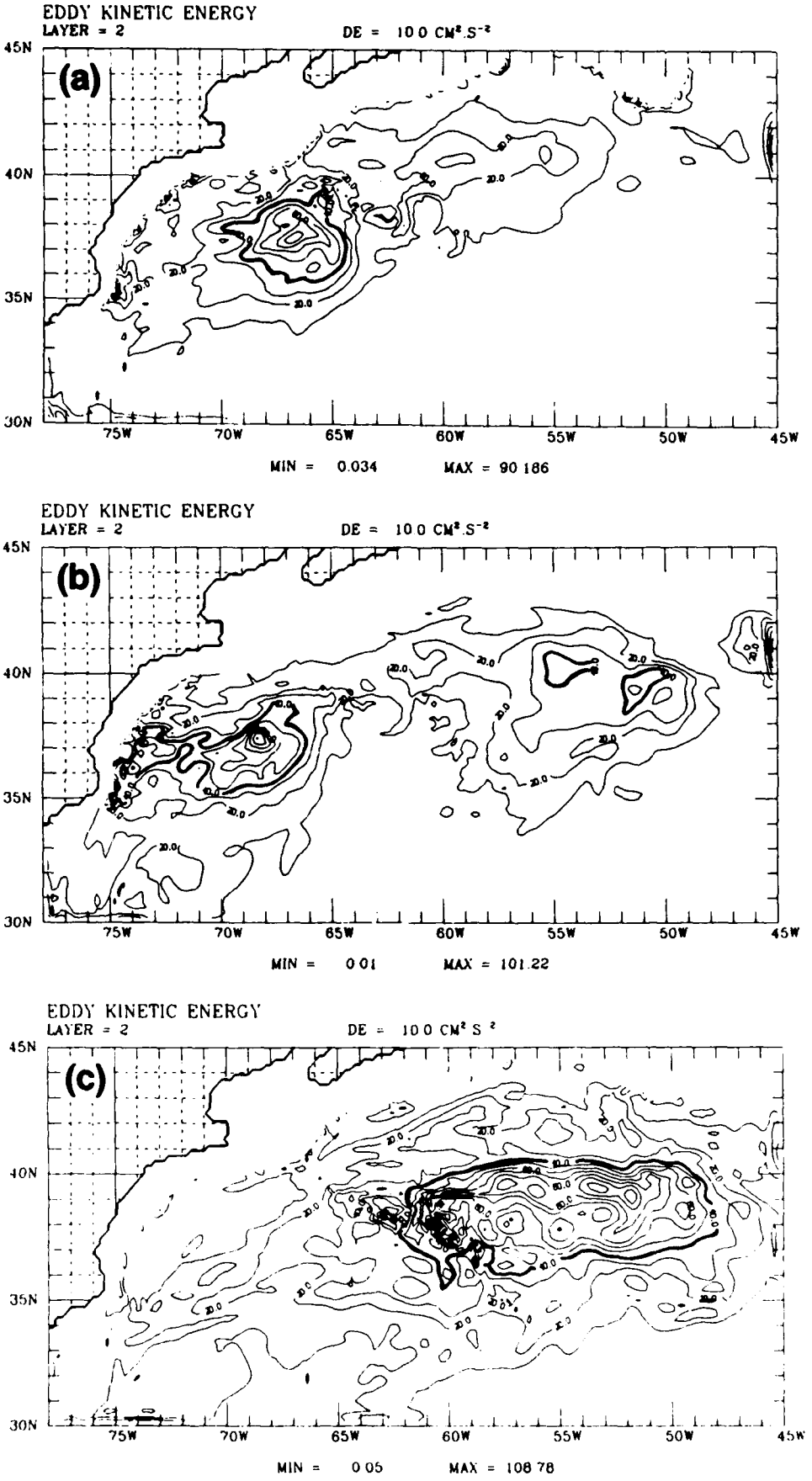

FIG. 12. EKE2 for (a) Experiment 4 (no DWBC), (b) Experiment 5a (20-Sv DWBC), and (c) Experiment 6 (40-Sv DWBC). Contour interval is 10 $cm^2 s^{-2}$ with the 40 $cm^2 s^{-2}$ contour indicated by a heavy solid line.

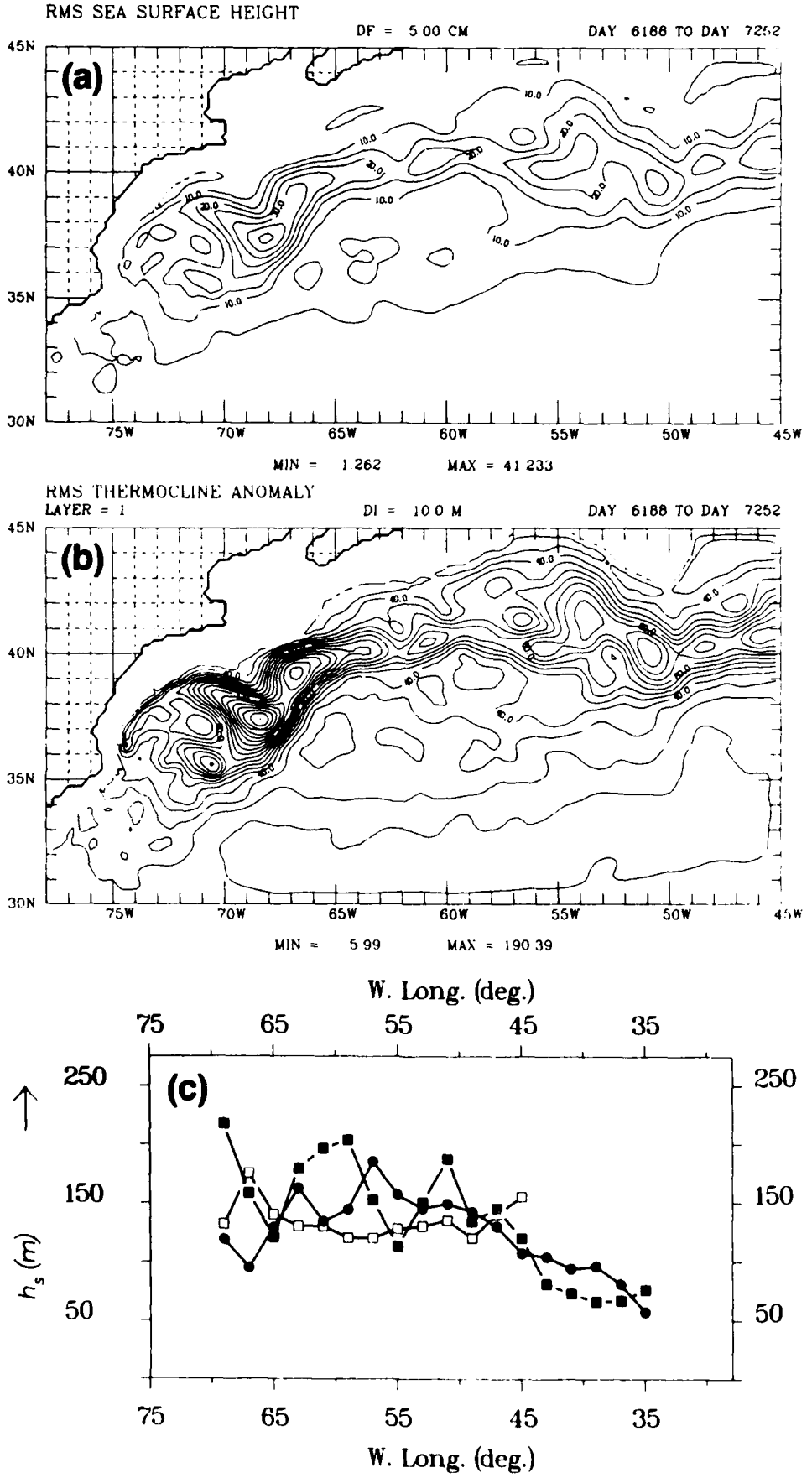

FIG. 13. (a) Root mean square of SSH for Experiment 5a. Contour interval is 5.0 cm. (b) Rms of thermocline anomaly. Contour interval is 10 m. (c) Rms of 15°C. isotherm from Dantzler (1977) at 37° and 39°N and maximum variability from model thermocline from Experiment 5b.

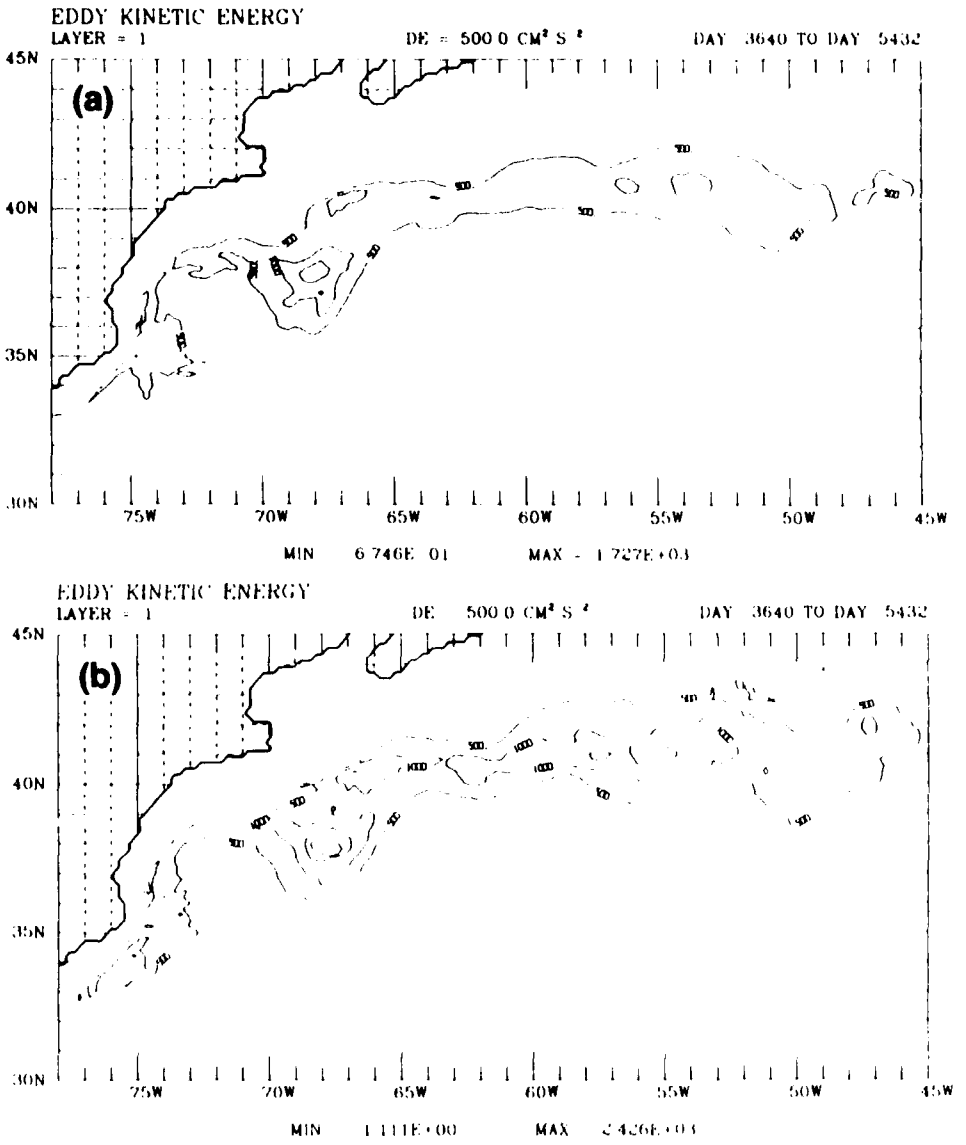

FIG. 14. EKE from (a) Experiment 5a and (b) Experiment 5b. Contour intervals are 500 cm² s⁻².

although the downstream decay appears more rapid in the drifter data than in the model results. As discussed above, the deep layer thickness, the lack of time dependence in the wind field and the constant inflow transport all contribute to the lower values in EKE from the model results. It is very likely that higher vertical and horizontal resolution in the model would improve the comparison with the data.

Figure 15 shows a histogram for the mass transport at 55°W for the (a) upper layer, (b) lower layer, and (c) total, averaged over one degree latitude bands. The recirculation zones are dramatically illustrated in these figures. Note that the total eastward transport, which includes a significant eddy-flux induced circulation, is 194 Sv between 39° and 41°N (recall the specified inflow at Cape Fear is 50 Sv). This is much larger than the total mean transport of 93 Sv at 55°W by Richardson (1985). However, the appropriately weighted difference between model upper and lower layer transports associated with the model Gulf Stream analogue yields a value (relative to the bottom) of 93 Sv, close to the 90 Sv estimate by McCartney et al. (1980) for the same calculation from observations at 55°W. (See also Schmitz 1980).

4. Summary and conclusions

We have applied a primitive-equation numerical model as a two-layer analogue of the Gulf Stream System to a limited area from Cape Hatteras to east of the Grand Banks (78°–45°W, 30°–48°N). In this initial paper six numerical experiments from a series of over 50 integrated to statistical equilibrium were selected for detailed description and intercomparison with ob-

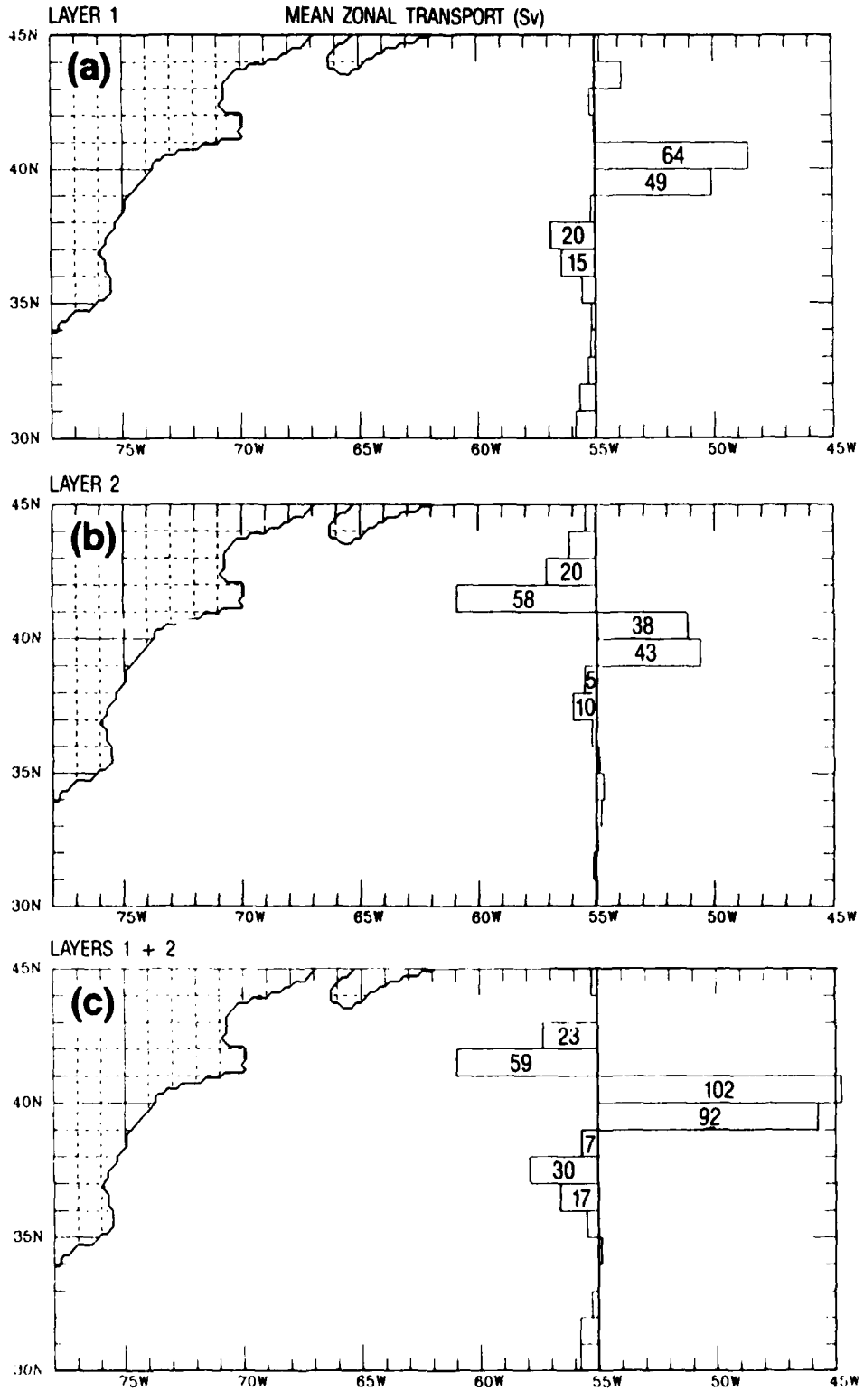

FIG. 15. Mean zonal transport histogram averaged over 2 degrees latitude bands at 55°W. from Experiment 5a for the (a) upper layer, (b) lower layer, and (c) total. Each degree longitude represents 10 Sv of transport.

servation. Experiment 1 consisted of a flat bottom regime driven by wind forcing only. Realistic inflow transport above the main thermocline was then prescribed for two different outflow specifications at the eastern boundary in Experiments 2 and 3. Three other model runs included (4) bottom topography, (5) a deep

western boundary current with 20 Sv total transport added to Experiment 4, and (6) increasing the Deep Western Boundary Current (DWBC) in Experiment 5 to 40 Sv.

Without a prescribed inflow (Florida Current Transport) the resulting velocity fields are much too weak, as expected. For a realistic inflow transport exiting at a fixed narrow outflow location both the mean and eddy fields are quite unrealistic. For an entirely open eastern boundary the modelled Gulf Stream System with realistic topography is more energetic at abyssal depths but is located too far north relative to observations. The addition of the DWBC moves the mean path of the midlatitude jet southward toward a more realistic configuration, shifting the region of increased abyssal EKE eastward thus improving the comparison with deep observations at 55°W. The 20 Sv DWBC experiment (Expt. 5) also yields a deep mean flow which corresponds to the observational data in several areas, including recirculations north and south of the Gulf Stream and a deep cyclonic gyre just to the east of the northern part of the NESC. Another deep cyclonic circulation at the foot of the continental rise centered near 37°N, 68°W and anticyclonic deep flows around several isolated topographic features such as the Corner Rise Seamounts and Bermuda are also indicated in the model results but as yet have little or no observational data to confirm them. The amplitudes of upper level eddy kinetic energies and the mean flow are within at least a factor of two of the data base and the model equivalent Gulf Stream transport at 55°W is potentially relevant. Additional model/data intercomparisons utilizing GEOSAT altimeter data, inverted echo sounders, and bottom pressure gauges are reported by Hallock et al. (1988).

These initial results are encouraging, but the need for future work is clear. To be examined further are problems associated with changing vertical and horizontal resolution (Are our two-layer results valid in the limit of continuous stratification?), model dynamics (How is the Northern Recirculation Gyre driven by eddy fluxes?), and model/data intercomparisons [Are model simulations of warm and cold ring generation, translation, and decay compatible with the observations of Auer (1987), Brown et al. (1986), and others?]. We do not discount the possibility that separation of the Gulf Stream could be better achieved by allowing surfacing of the fluid interface. A surfaced or ventilated thermocline appears to be a crucial component in a successful thermocline theory (Luyten et al. 1983), and Veronis (1981) have argued that realistic separation of midlatitude western boundary currents from the coast must necessarily include surfacing of the thermocline as well. Western boundary currents forced out to sea between wind gyres of opposite sign are, in this view, qualitatively different because the thermocline does not surface. Nevertheless, we believe the key issue discussed in this paper, the influence of the DWBC on the Gulf Stream, is relevant to either regime. Because of the efficiency and relative simplicity of this model we have begun to examine these and related problems using computational resources widely available today.

Acknowledgments. This paper is a contribution to the Regional Energetics Experiment (REX) program sponsored by the Office of Naval Research to the Naval Ocean Research and Development Activity under the Accelerated Research Initiatives "Ocean Dynamics from Altimetry" (ONR 32-05-3F) and the "GEOSAT Exact Repeat Mission" (ONR 32-05-3G) (supporting J.D.T.). W.J.S. was supported in this investigation by the ONR and the Institute for Naval Oceanography. The INO is sponsored by the Navy and administered by the Office of the Chief of Naval Research. Thanks are due to Harley Hurlburt, Jim Mitchell, George Heburn, John Kindle, and Alan Wallcraft for assistance in model development and analysis and many aspects of manuscript preparation. Comments from Bill Holland, Nelson Hogg, John Bane, David Adamec, and two anonymous reviewers were also extremely helpful. We are grateful to Nelson Hogg and Phil Richardson for the use of previously published figures. Appreciation is extended to Lina Lo and Woody Woodyard of JAYCOR for programming assistance and figure preparation. Calculations were performed on the Cray XMP-24 at the Naval Research Laboratory in Washington, DC, the CDC Cyber 205 at Florida State University, and on the Institute for Naval Oceanography's VAX-8800 at the Stennis Space Center, Mississippi. Graphics software was in part provided by the National Center for Atmospheric Research (sponsored by the National Science Foundation).

APPENDIX A

List of Symbols

A	horizontal eddy viscosity
C_b	coefficient of bottom friction
f	Coriolis parameter
g	acceleration due to gravity
g'	reduced gravity, equal to $g(\rho_2 - \rho_1)/\rho$
H_i	thickness of layer i at rest
h_i	instantaneous layer thickness of the ith layer
p_i	density normalized pressure for layer i
t	time
$\mathbf{v}_i$	current velocity in layer i with x-directed component u_i and y-directed component v_i
$\mathbf{V}_i$	volume transport, $h_i\mathbf{v}_i$
$\mathbf{v}_{ig}$	geostrophic current velocity
x, y, z	tangent plane Cartesian coordinates: x positive eastward, y positive northward, and z positive upward
Δt	time step in the numerical integration

Δx, Δy horizontal grid increments for each independent variable

η_1 free surface height anomaly (FSA), height of the free surface above its initial elevation

ρ, ρ_i densities of seawater

τ_i^x, τ_i^y x- and y-directed tangential stresses at the top (i) and bottom ($i + 1$) of layer i respectively

APPENDIX B

The Gulf Stream Model

Consider a stably stratified Boussinesq fluid with a free surface and a fixed density contrast specified between immiscible layers. All thermodynamic effects are neglected. Each interface between fluid layers is thus an isopycnal surface. While the actual system of equations is solved on an earth-sized spherical geometry, for simplicity we will use Cartesian geometry in the discussion below. In transport form the vertically integrated equations of motion used in the models are

$$\frac{\partial \mathbf{V}_i}{\partial t} + (\nabla \cdot \mathbf{V}_i + \mathbf{V}_i \cdot \nabla)\mathbf{v}_i + \mathbf{k} \times f\mathbf{V}_i = -h_i \nabla P_i + \rho^{-1}(\tau_i - \tau_{i+1}) + A\nabla^2 \mathbf{V}_i, \quad \text{(B.1)}$$

$$\frac{\partial h_i}{\partial t} + \nabla \cdot \mathbf{V}_i = 0, \quad \text{(B.2)}$$

where

$$\nabla = \frac{\partial}{\partial x}\mathbf{i} + \frac{\partial}{\partial y}\mathbf{j},$$

$$P_i = g\nabla\eta_1 - g\sum_{j=1}^{i-1} \epsilon_{ij} \nabla h_j,$$

$$\epsilon_{ij} = (\rho_i - \rho_j)/\rho_i,$$

$$\mathbf{V}_i = h_i \mathbf{v}_i = h_i(u_i \mathbf{i} + v_i \mathbf{j}),$$

$$\tau_i = \tau_i^x \mathbf{i} + \tau_i^y \mathbf{j}. \quad \text{(B.3)}$$

See appendix A for symbol definitions.

In the two-layer experiment discussed here, $i = 1, 2$ with τ_2 (interfacial stress) set to zero and τ_3 (bottom stress) quadratic in velocity, i.e.

$$\tau_3 = C_d |\mathbf{v}_2| \mathbf{v}_2.$$

This layered model, with transports U, V as dependent variables, handles strongly sloping topography especially well, so long as it is confined to the lowest layer. The topography appears multiplicatively in the pressure gradient term and is differentiated only to the extent that it affects the velocity field in the advective terms. When large-amplitude topography is introduced, restrictions on the time step and the eddy coefficient are affected only to the extent that the topography determines the amplitude of the velocity field (advective CFL condition) and the grid interval Reynolds number. The continuity equation is linear when written in transport form, thus avoiding complications from the nonlinear advective term when layer thickness and velocity are used as variables.

Except at the inflow and outflow ports, the walls are rigid and the no-slip condition is prescribed on the tangential flow. At inflow the profile of transport $\mathbf{V}_i$ is prescribed as a parabolic function. Because the current is nearly geostrophic, the upper layer velocity maximum is to the left of the center of the jet when facing downstream. The normal flow at the outflow port is self-determined with the integral constraint that the total transport out from each layer match the inflow at all times.

The numerical design of the model is similar to that described by Hurlburt and Thompson (1980) and will not be rewritten here. However, differences in methodology for handling the open boundary conditions are described below. The flow at the open boundaries are predicted in three steps:

First, a modified Orlanski (1976) radiation condition is used such that for each component of the transport

$$q_B^{t+1} = \left[\left[1 - \frac{\Delta t c}{\Delta x}\right] q_B^{t-1} + \left(\frac{2\Delta t}{\Delta x}\right) c q_{B-1}^t\right] \Big/ \left(1 + \frac{\Delta t c}{\Delta x}\right) \quad \text{(B.4)}$$

where B refers to the outflow boundary, $B - 1$ is one grid point interior to the boundary,

$$c = \min\left(\frac{\Delta x}{\Delta t}\right), \max(c_k, \bar{u}_{0k}),$$

$\bar{u}_{0k}$ is the mean inflow speed, and the phase speed c_k is determined locally for each wave mode. There are several ways to determine the local phase speed, c_k, but we have found that $c_k = \bar{u}_{0k}$ is effective for outflow for the Gulf Stream.

Second, if inflow is predicted at an outflow point, a linear implicit drag is applied. This is required because in an open boundary condition with self-determined flow the mean is constrained. In the case of an east–west boundary, deviations from the mean flow are somewhat constrained by the tendency to form a Sverdrup interior (Hurlburt and Thompson 1973). However, for a north–south oriented boundary it is possible to develop a recirculation at the eastern open boundary driven by the eddy-fluxes from the Gulf Stream. This mode can grow unrealistically large unless there is a "brake" on the inflow component of the recirculation at the outflow boundary (Hurlburt and Thompson 1980). The damping time scale (one day) effectively inhibits an unrealistic recirculation at 45°W.

Finally, the x-component of transport is uniformly accelerated or decelerated such that total inflow mass transport is matched by total outflow transport for that time step. The outflow boundary condition does not

use any interior values at time level $n + 1$, so it can provide the solver with the boundary information on transport required at the ports. We can then solve the Helmholtz equations for $h_{i,j}^{n+1}$. Once we have $h_{i,j}^{n+1}$, the semi-implicit calculation of $U_{i-1/2,j}^{n+1}$ and $V_{i,j-1/2}^{n+1}$ in the interior can be completed.

The behavior of the open boundary condition has been remarkably good. Comparisons by Heburn and Hurlburt (personal communication) of results from a Caribbean model with the radiation condition used here and an identical experiment using the boundary condition of Hurlburt and Thompson (1980) without the Coriolis term show good agreement. Strong jets pass through, as do eddies. Gravity wave reflections are not a dominant component of the model solutions nor is extra damping required on the outflow boundary.

The Helmholtz equations are solved using a vectorized variant of the capacitance matrix technique (Busbee et al. 1971) for homogeneous Neumann boundary conditions one-half grid distance outside the h grid on a general non-rectangular geometry (Wallcraft 1980). Each solution requires two calls to a variant of Hockney's (1965) method developed by Daniel Moore (Imperial College, London) and Alan Wallcraft for rectangular regions.

REFERENCES

Adamec, D., 1988: Numerical simulations of the effects of seamounts and vertical resolution on strong ocean flows. *J. Phys. Oceanogr.*, **18**, 258–269.

Auer, S. J., 1987: Five-year climatological survey of the Gulf Stream System and its associated rings. *J. Geophys. Res.*, **92**, 11 709–11 726.

Bogue, N. M., R. X. Huang and K. Bryan, 1986: Verification experiments with an isopycnal coordinate model. *J. Phys. Res.*, **16**, 985–990.

Boris, J. P., and D. L. Book, 1973: Flux-corrected transport. Part I: SHASTA, A fluid transport algorithm that works. *J. Comput. Phys.*, **11**, 38–69.

Brown, O. B., P. C. Cornillon, S. R. Emmerson and H. M. Carle, 1986: Gulf Stream warm rings: a statistical study of their behavior. *Deep-Sea Res.*, **33**, 1459–1473.

Busbee, B. L., F. W. Dorr, J. A. George and G. H. Golub, 1971: The direct solution of the discrete Poisson equation on irregular regions. *SIAM J. Num. Anal.*, 722–736.

Cox, M. D., 1985: An eddy resolving numerical model of the ventilated thermocline. *J. Phys. Oceanogr.*, **10**, 1312–1324.

Dantzler, H. L., 1977: Potential energy maxima in the tropical and subtropical North Atlantic. *J. Phys. Oceanogr.*, **7**, 512–519.

Douglas, B. C., R. E. Cheney and R. W. Agreen, 1983: Eddy energy of the Northwest Atlantic and Gulf of Mexico determined from GEOS 3 altimetry. *J. Geophys. Res.*, **88**, 9595–9604.

Fisher, A., 1977: Historical limits of the northern edge of the Gulf Stream. *Gulfstream*, **3**, 265–273.

Halliwell, G. R., Jr., and C. N. K. Mooers, 1983: Meanders of the Gulf Stream downstream from Cape Hatteras. *J. Phys. Oceanogr.*, **13**, 1275–1292.

Hallock, Z. R., J. L. Mitchell and J. D. Thompson, 1988: Sea surface height variability near the New England Seamounts: an intercomparison among in situ observations, GEOSAT altimetry, and numerical simulation. *J. Geophys. Res.*, in press.

Harrison, D. E., 1982: On deep mean flow generation mechanisms and the abyssal circulation of numerical model gyres. *Dyn. Atmos. Oceans*, **6**, 135–152.

Heburn, G. W., and H. E. Hurlburt, 1988: A numerical study of mesoscale variability in the eastern Caribbean Sea. (submitted to *J. Phys. Oceanogr.*).

Hellerman, S., and M. Rosenstein, 1983: Normal monthly wind stress over the world ocean with error estimates. *J. Phys. Oceanogr.*, **13**, 1093–1104.

Hockney, R. W., 1965: A fast direct solution of Poisson's equation using Fourier Analysis. *J. Assoc. Comput. Mach.*, **12**, 95–113.

Hogg, N. G., 1983: A note on the deep circulation of the western North Atlantic: Its nature and causes. *Deep-Sea Res.*, **30**, 945–961.

——, and H. Stommel, 1985: On the relation between the deep circulation and the Gulf Stream. *Deep-Sea Res.*, **32**, 1181–1193.

——, R. S. Pickart, R. M. Hendry and W. J. Smethie, Jr., 1986: The northern recirculation gyre of the Gulf Stream. *Deep-Sea Res.*, **33**, 1139–1165.

Holland, W. R., and L. B. Lin, 1975: On the generation of mesoscale eddies and their contribution to the oceanic general circulation. Part I: A preliminary numerical experiment. *J. Phys. Oceanogr.*, **5**, 642–657.

——, and W. J. Schmitz, 1985: Zonal penetration scale of midlatitude jets. *J. Phys. Oceanogr.*, **15**, 1859–1875.

Hurlburt, H. E., 1984: The potential for ocean prediction and the role of altimeter data. *Mar. Geod.*, **8**, 17–66.

——, and J. D. Thompson, 1980: A numerical study of Loop Current intrusions and eddy shedding. *J. Phys. Oceanogr.*, **10**, 1611–1651.

——, and ——, 1984: Preliminary results from a numerical study of the New England Seamount chain influence on the Gulf Stream. *Proc. of the Workshop on Predictability of Fluid Motions*. Amer. Inst. Phys. G. Hollaway, Ed.

——, and ——, 1973: Coastal upwelling on a β-plane. *J. Phys. Oceanogr.*, **3**, 16–32.

Lai, D. Y., 1984: Mean flow and variabilities in the Deep Western Boundary Current. *J. Phys. Oceanogr.*, **14**, 1488–1498.

Luyten, J. R., J. Pedlosky and H. Stommel, 1983: The ventilated thermocline. *J. Phys. Oceanogr.*, **13**, 292–309.

Marsh, J. G., R. E. Cheney, J. J. McCarthy and T. V. Martin, 1984: Regional mean sea surface based upon GEOS-3 and Seasat altimeter data. *Mar. Geod.*, **8**, 385–402.

McCartney, M. S., L. V. Worthington and M. E. Raymer, 1980: Anomalous water mass distribution at 55 W in the North Atlantic in 1977. *J. Mar. Res.*, **38**, 147–172.

Mellor, G. L., C. R. Mechoso and E. Keto, 1982: A diagnostic calculation of the general circulation of the Atlantic Ocean. *Deep-Sea Res.*, **29**, 1171–1192.

Niiler, P. P., and C. J. Koblinsky, 1985: A local time dependent Sverdrup balance in the Northeast Pacific. *Science*, **229**, 754–756.

Olbers, D. J., M. Wenzel, and J. Willebrand, 1985: The inference of North Atlantic circulation from climatological hydrographic data. *Rev. Geophys.*, **23**, 313–356.

Orlanski, I., 1976: A simple boundary condition for unbounded hyperbolic flows. *J. Comput. Phys.*, **21**, 251–269.

Richardson, P. L., 1981: Gulf Stream trajectories measured with free-drifting buoys. *J. Phys. Oceanogr.*, **11**, 990–1010.

——, 1983: Eddy kinetic energy in the North Atlantic from surface drifters. *J. Geophys. Res.*, **88**, 4355–4367.

——, 1985: Average velocity and transport of the Gulf Stream near 55 W. *J. Mar. Res.*, **43**, 83–111.

Richardson, W. S., W. J. Schmitz and P. P. Niiler, 1969: The velocity structure of the Florida Current from the Straits of Florida to Cape Fear. *Deep-Sea Res.*, **16**(Suppl.), 225–231.

Riser, S. C., H. Freeland and H. T. Rossby, 1978: Mesoscale motions near the deep western boundary current of the North Atlantic. *Deep-Sea Res.*, **25**, 1179–1191.

Schmitz, W. J., 1980: Weakly depth-dependent segments of the North Atlantic circulation. *J. Mar. Res.*, **38**, 111–133.

——, 1984: Abyssal eddy kinetic energy in the North Atlantic. *J. Mar. Res.*, **42**, 509–536.

——, and W. R. Holland, 1982: A preliminary comparison of selected numerical eddy-resolving general circulation experiments with observations. *J. Mar. Res.*, **40**, 75–117.

——, and ——, 1986: Observed and modelled mesoscale variability near the Gulf Stream and Kuroshio Extension. *J. Geophys. Res.*, **91**, 9624–9638.

——, W. R. Holland and J. F. Price, 1983: Mid-latitude mesoscale variability. *Rev. Geophys. Space Phys.*, **21**, 1109–1119.

Stommel, H. M., 1958: The abyssal circulation. *Deep-Sea Res.*, **5**, 80–82.

Swallow, J. C., and L. V. Worthington, 1961: An observation of a deep counter-current in the western North Atlantic. *Deep-Sea Res.*, **8**, 1–19.

Thompson, J. D., 1986: Altimeter data and geoid error in mesoscale ocean prediction: some results from a primitive equation model. *J. Geophys. Res.*, **91**, 2401–2417.

——, and H. E. Hurlburt, 1982: A numerical study of the influence of the New England Seamount Chain on the Gulf Stream: Preliminary results. *Proc. Workshop on Gulf Stream Structure and Variability*, Univ. of N.C., Chapel Hill, J. M. Bane, Jr., Ed., Office of Naval Research, 346–352.

Van Wyckhouse, R. J., 1979: Synthetic Bathymetric Profiling System, Volume I: Data sources and data preparation. Naval Ocean Research and Development Activity, NSTL, Ms., NORDA Tech. Note 35.

Veronis, G., 1981: Dynamics of large-scale ocean circulation. *Evolution of Physical Oceanography*, B. A. Warren and C. Wunsch, Eds., The MIT Press, 157 pp.

Wallcraft, A. J., 1980: Capacity matrix techniques. Ph.D. Thesis, University of London, Imperial College, 267 pp.

——, and J. D. Thompson, 1984: Ocean modelling and drifters. *1984 Drifting Buoy Workshop Proceedings*. Nat. Space Tech. Lab, Miss. Mar. Tech. Soc., 81–98.

Worthington, L. V., 1962: Evidence for a two gyre circulation in the North Atlantic. *Deep-Sea Res.*, **9**, 51–67.

Wunsch, C., and B. Grant, 1982: Towards the general circulation of the North Atlantic Ocean. *Progress in Oceanography*, Vol. 11, Pergamon, 1–59.

Wyrtki, K., L. Magaard and J. Hagar, 1976: Eddy energy in the ocean. *J. Geophys. Res.*, **81**, 2641–2646.